Università degli Studi di Padova

Department of Molecular Medicine
University of Padua

Ph.D. COURSE IN: Molecular Medicine
CURRICULUM: Regenerative Medicine
SERIES: XXX

Dissecting the molecular function of mutant Huntingtin with stem cells

Thesis written with the financial contribution of Telethon Foundation

Coordinator: Prof. Stefano Piccolo
Supervisor: Prof. Graziano Martello

Ph.D. student: Giorgia Maria Ferlazzo

Forse è ormai abitudine, o più attitudine, personalissima, ad andare avanti sempre, sempre e comunque, nonostante tutto e tutti e raggiungere quello che ti sei messo in testa, costi quel che costi. Sì, ci vuole tanta volontà, determinazione… è forza, è istinto… sicuramente innato sì, ma se ce l'hai fatta, se ce la fai, non deve essere scontato "che tanto ce la fai sempre".

E in alcuni momenti ho fermamente creduto di non farcela, non per malavoglia, quanto perché davanti a me c'era qualcosa di imponente, immensamente difficile, smisurato in confronto alle mie possibilità e capacità. Almeno per quelle che credevo di avere. E invece mi sono piacevolmente dovuta ricredere. Su me stessa. All'inizio solo piccoli passi e poi un passo dopo l'altro, un giorno dopo l'altro, dal fare ogni giorno il possibile, senza rendermene conto mi sono ritrovata a fare ciò che pensavo fosse impossibile. Ho sperimentato la forza della pazienza. Novità assoluta per me! E ce n'è voluta davvero parecchia di pazienza, con me stessa soprattutto. Preamboli e considerazioni esistenziali a parte, tutto può essere riassunto da una parola semplice semplice, che stupidamente uso troppe poche volte.

Grazie.

Non ce l'avrei mai fatta in questi 3 anni, non da sola.

Grazie a mia madre, a mio padre e a mio fratello, grazie prima di ogni cosa alla mia famiglia, siete in tutto quello che sono e che faccio, da sempre e per sempre dalla mia parte, senza mai aver fatto pesare le mie scelte, anche se sofferte e non sempre condivise.

Grazie ad Antonio, colui che mi ha insegnato a lavorare in questo campo e che inconsciamente è stato l'artefice del mio trasferimento a Padova.

Un grazie immenso a Donatella e Daniele, e a Simone, per avermi subito accolto "come una di famiglia", addolcendo l'ennesimo trasferimento e sostenendomi materialmente in questi anni.

Grazie a tutto il laboratorio, primo fra tutti Graziano, per avermi dato fiducia fin dall'inizio quando io stessa non me ne sarei data. Grazie per avermi guidato in questo percorso, concedendomi spazio e tempo di potere essere anche io a scegliere, pur non sempre la cosa giusta, e di capire e crescere professionalmente e personalmente.

Un grazie particolare ad Elena, per la sua infinita disponibilità, sei stata per me di grande supporto tecnico e morale.

Grazie a Irene, alla sua sensibilità e generosità, grazie per avere "addolcito" molte lunghe giornate.

Grazie a tutti i ragazzi, da chi è arrivato a Padova quasi in contemporanea, Marco, a chi si è via via aggiunto, a Mattia, Cristina fino a Valentina, dando propositività e stimoli sempre nuovi.

Un doveroso ringraziamento a parte va a chi questo percorso lo ha fatto fianco a fianco a me, a Riccardo, "compagnetto" di banco, di mille caffè alternati a spritz, di scleri pre-scadenze e follie burocratiche.

Grazie ad Arianna, alla sua energia contagiosa e alle macumbe precedenti lo sviluppo dei blot, e a tutto il "vicinato" di lab, a Sirio e alle dupontine Giulia, Patrizia e Irene, sempre disponibili a dare anche più di una mano.

Grazie alle mie galline padovane, a Francesca, la mia gemella diversa, a Chiara e Margherita e tutta casa madonnetta, sempre calda e accogliente; grazie ad Alessandra, compagna di avventure, grazie a Cecilia che "passo anche al volo, solo per un abbraccio" e a Lucia che solo un messaggio e scatta il sorrisone. Grazie a Ilaria, amica sincera e leale nel momento del vero bisogno.

Grazie a chi c'è praticamente da sempre e sempre rimane a sopportarmi e supportarmi, non contando più i chilometri e gli anni. Grazie a Manu, compagna di vita, a mia sorella Silvia, a Dario, Ciccio, Fede, Chiara, che ogni volta che "scendo" è sempre una grande meravigliosa festa.

Grazie a chi è entrato nella mia vita più recentemente, ritagliandosi un posto unico e speciale, ad Elisa, Angela, Federica, Valentina e Ornella, perché Bologna come Milano, Parma o Palermo, Leuven può essere "casa" quanto Barcelona, basta essere insieme e ovunque sono risate in apnea e tavolate "auguriose".

Grazie anche a chi c'è stato fino ad un certo punto, ma poi ha preferito non esserci più, restituendomi consapevolezza di me stessa e lasciandomi serenità di scelta.

Un pensiero e un grazie infine per chi non è potuto esserci più, ma sento sempre accanto a me.

Grazie a tutti voi. Grazie di cuore. Questo non è solo un mio traguardo, ma è un po' di ognuno di voi. In realtà non lo chiamerei nemmeno traguardo. Perché è già un nuovo inizio. Fine o inizio che sia, non sarà nulla se non lo si condivide.

Index

Abstract

Huntington's disease (HD) is an incurable neurodegenerative disorder caused by CAG expansion in Htt locus leading to the loss of striatal neurons.

Here, I described a full methodology to perform a gain-of-function screening with Embryonic Stem (ES) cells, that I used to obtain an understanding of the molecular mechanism of action of mutant Htt protein. Differently from conventional screenings for HD, the approach I developed is based on the use of mammalian (mouse) ES cell system and takes advantage of state of the art technology of piggyBac vector for achieving random genome-wide mutagenesis.

A preliminary screening for regulators of SRF pathway, advantaged by availability of a fluorescent reporter for SFR activity, was set up in order to acquire technical expertise required for the screening procedure.

Subsequently, I carried out gain-of-function screen on ES cell lines stably expressing mutant Htt (Q128 Htt) characterized them and observed impaired proliferation and increased sensitivity to MG132 and Tamoxifen stressors. I performed mutagenesis on Q128 Htt cells and screened for rare clones surviving to mutant Htt toxicity thanks to over-activation of some genes. By Splinkerette-PCR, I succeeded in the identification of a set of candidate genes that are potentially able to reduce the toxic effects of mutant Htt. After extensive validations, Mtf1, Kdm5b and Arid1b gene were confirmed as *bonafide* suppressors of mutant Htt toxicity. Such genes will be also tested in more relevant model systems, such as immortalized striatal neurons expressing mutant Htt and animal models and will represent novel promising therapeutic targets for HD.

Sommario

La Corea di Huntington (o Huntington Disease, HD) è una rara patologia neurodegenerativa che attualmente non ha alcuna cura. La malattia è causata dall' espansione della tripletta CAG nel gene HTT. Tale mutazione è responsabile della produzione della proteina Huntingtin mutata che risulta essere citotossica in particolare per i neuroni dello striato.

Lo scopo del progetto è eseguire uno screening funzionale utilizzando cellule embrionali staminali (ES) per meglio comprendere i meccanismi molecolari attraverso i quali la proteina Huntingtin agisce.

Uno screening preliminare per regolatori della via di segnalazione di SRF, facilitato dall'utilizzo di un costrutto fluorescente in grado di monitorarne l'attività, mi ha permesso di acquisire tutte le competenze tecniche necessarie per lo sviluppo della procedura di screening.

Una volta ottimizzata la tecnica, ho realizzato lo screening per HD. Ho innanzitutto generato cellule ES che esprimono Huntingtin mutata e osservato difetti nella proliferazione ed aumentata sensibilità ad agenti stressanti. Ho poi eseguito mutagenesi inserzionale mediata da retrotrasposoni che si integrano casualmente nel genoma e determinano l'attivazione di geni fiancheggianti. Tali geni sono stati identificati come potenziali riduttori degli effetti tossici di Htt mutata. I 3 candidati più promettenti (Mtf1, Kdm5b e Arid1b) saranno a breve testati in modelli di malattia quali neuroni stratali ed Zebrafish transgenici.

Introduction

Huntington's Disease

Huntington's disease (HD) is an inherited neurological disorder caused by expansions of CAG triplet within coding region of the Huntingtin (HTT) gene (The Huntington's Disease Collaborative Research Group, 1993), thus resulting in the formation of a mutant huntingtin protein containing a stretch of glutamine residues at NH_2 terminus.

The consequence of HD single genetic lesion is severe brain degeneration, leading to dementia and motor dysfunction due to loss of a subset of neurons in the striatum (Reiner A, 1988). The wild-type (wt) huntingtin protein includes up to 35 CAG repeats (Figure 1.A, top). Htt is a 348-kDa ubiquitary protein, widely expressed in different cells of body (Di Figlia M, 1995). Moreover, at the subcellular level, it has been found in the nucleus and several cytoplasmic organelles (Hilditch-Maguire P, 2000; Hoffner G, 2002).

Murine Htt is essential in early stages of development as its complete loss causes embryonic lethality before the formation of the neural tube (Duyao MP, 1995; Nasir J, 1995; Zeitlin S, 1995). In adult brain, Htt is implicated in the resistance to apoptotic stimuli and in the transcriptional control of BDNF and other RE1/NSRE regulated genes (Conforti P, 2013; Nucifora FC, 2001; Rigamonti D, 2000; Lo Sardo V, 2012).

The mutated version of Htt (mHtt) contains an aberrant number (>36) of CAG repeats (Figure 1.A, bottom) leading to the development of symptoms in patients between 35 and 50 years of age. The higher the number of CAG repeats is, the more severe HD will be, and the earlier the symptoms of the disease will appear (Conneally PM, 1984). More than 60 CAG repeats are associated with a disease onset during childhood or adolescence (juvenile HD).

HD is not simply caused by the loss of one allele of HTT gene, but rather by new functions acquired by mHtt, overviewed in Figure 1.B (Zuccato C, 2010; Ross CA and Tabrizi SJ, 2011). Mutant protein undergoes proteolytic processing (Goldberg YP, 1996; Kim KJ, 2001; Wellington CL, 2002) and the resulting toxic fragments aggregate and

accumulate in cellular compartments (Di Figlia M, 1997; Davies SW, 1997). Moreover, mHtt induces neurodegeneration through abnormal interactions with other proteins in the cytoplasm, causing impairment of calcium signaling and mitochondrial damage (Panov AV, 2002) and inhibition of protein clearance pathways (Bennet EJ, 2007). Misregulation of the transcriptional program is reported as a consequence of translocation of toxic fragments into the nucleus (Zuccato C, 2001; Dunah AW, 2002; Benn CL, 2008). mHtt protein causes alteration of vesicular recycling, excitoxicity and cortico-striatal synapse dysfunction, increasing both glutamate release from cortical neurons and glutamate receptor activity in medium spiny neurons (reviewed in Sepers MD and Raymond LA, 2014). However, it is not known which of these changes play a causal role in HD and which other are simply consequences of the general impairment of cellular homeostasis. Despite all the knowledge acquired of HD pathogenesis, no effective therapeutic intervention is yet available.

Genetic screenings and models for HD

Genetic screens to identify genes involved in the cytotoxic effects of mHtt have been carried out in model systems such as *Saccaromices cerevisiae* and *Caenorhabditis elegans* (Giorgini F, 2005; Nollen EAA, 2004). These studies successfully identified new therapeutic targets, but suffer from limitations such as difficulty in the identification of mammalian homologues of the newly identified genes and the time required to generate and screen libraries of mutants. Still, these screens have proven successful, allowing the identification of compounds that ameliorated neurodegeneration in mouse animal models of HD (Zwilling D, 2011).

A similar experimental approach carried out in a mammalian cellular system would be a better option, overcoming restrictions due to the use model systems evolutionary far from mammalians. *In vitro* cellular models for HD expressing wild-type or mutant Htt have been extensively used to investigate disease mechanisms or to test the effect of drugs (Rigamonti D, 2007; Sipione S and Cattaneo E, 2001; Varma H, 2007). More recently, human Pluripotent Stem cells (hPSC) were isolated from HD embryos (Verllinsky Y, 2005; Niclis JC, 2009) and induced Pluripotent Stem (iPS) cells have been successfully derived from HD patients (HD iPSC Consortium, 2012). Those novel *in-vitro*

human stem cell models of HD will represent a great resource allowing the study of pathogenic mechanisms in human cells. Remarkably, HD-iPS cells might be used in biomedical and translational HD research. Nevertheless, cell-intrinsic features of hPSC such as technical difficulties of genomic modifications and low single-cell survival rates have limited their use for genetic screenings.

My aim is to carry out a genome-wide genetic screen in order to identify new genes whose over-activation will suppress the detrimental effects of mHtt. Such genes will represent novel promising therapeutic targets. In order to do this, I chose to use a specific cellular model: murine Embryonic Stem (mES) cells expressing mutant huntingtin. The choice of this particular system is justified by the unique ease of genetic manipulation of mES cells, their intact genome and their unique capacity to differentiate into neurons.

Genome-wide screen with mouse Embryonic Stem cells

Mouse embryonic stem cells were isolated from the inner cell mass (ICM) of pre-implantation (~E3.5) embryo (Evans MJ and Kaufman MH, 1981; Martin GR, 1981). ES cells capture many features of the epiblast and are defined *pluripotent*, as they can differentiate into the three germ layers of the embryo when injected in recipient blastocysts. They could be expanded almost indefinitely in defined culture conditions (Ying QL, 2008), retaining pluripotency and genomic stability (Martello G and Smith A, 2014). ES cells possess several unique features that make them particularly attractive as model system: low cost and simple cell culture conditions, high proliferative rate, homogeneity of cellular phenotype. Furthermore, their high amenability to genome modification enables the generation of large-scale mutant libraries, which can be subsequently used for genetic screens (Chambers I, 2003; Vierbuchen T, 2010). Moreover, the use of ES cells allows obtaining either differentiated cell types of interest or entire animal models carrying mutations in the newly identified genes. Of note, mouse ES cells have been already used to study Htt distribution in cellular organelles (Hilditch-Maguire P, 2000) and the cellular effects of mHtt, such as deregulation of transcription (Biagioli M, 2015) or metabolism (Isamouglu I, 2014),

increased oxidative stress and consequent DNA damage accumulation at CAG repeats (Jonson, I 2013).

A general approach to perform genetic screening using ES cells is summarized in Figure 2.A. A genetic screen consists of 4 main experimental steps (Li MA, 2010):

1) Genome-wide mutagenesis and generation of a mutant library;
2) Phenotypic selection of mutants of interest;
3) Identification of the mutated genes conferring the phenotype of interest;
4) Functional validation of candidate genes.

The basic principle of a forward genetic screen is to assign the function of a gene by the analysis of the phenotype resulted from alterations in its activity. In this case the aim is to perform a gain-of-function screening in which genes are over-activated. The available tools allowing random activation of genes are either retroviral or retrotransposon vectors containing strong promoters. Such vectors are both able to stably integrate into the host genome and activate flanking genes. In addition, their site of integration can be used as a unique molecular tag, facilitating the identification of the mutated loci.

Retroviruses have been amply used for transduction of ES cells (Guo G, 2004; Trombly MI, 2009; Wang and Bradley, 2007). However, analysis of pattern of integrations of retroviral vectors (Hansen GM, 2008) revealed that their integrations have a non-random distribution into the genome, thus limiting their use for genome-wide screens. Moreover, retroviral vectors are rapidly silenced in ES cells.

Recently, retrotransposons such as piggyBac (pB) vectors were adopted for efficient and stable expression of transgene of interest in mammalian cells (Liang Q, 2009; Wu SC, 2006; Guo G, 2009). Retrotransposons are DNA elements that can mobilized into the genome via a “cut and paste” mechanism (Figure 2.B). Transposition is catalyzed by a transposase enzyme that recognizes transposon-specific inverted terminal repeat sequences (ITRs) located on both ends of the pB vector, i.e. transposon vectors can be designed to carry any gene of interest flanked by ITR repeats. Transfection of a pB vector, in the presence of the transposase (supplied in trans from a separate expression vector), leads to random integration into TTAA sites that are extremely

abundant in the genome. Upon integration, TTAA sequence duplicates at both ends of the transposon (target-site duplication). Transient transfection of the transposase allows traceless excision of pB vector and restores the original genomic TTAA sequence (Yusa K, 2009).

Compared to retroviral vectors, pB integrations have resulted to be less biased (Wang W, 2008). Importantly, pB vectors do not undergo silencing in ES cells. Another advantageous feature of pB vectors is that there is no cargo limit, thus allowing the accommodation of highly complex and modular DNA sequence between ITRs. Moreover, the design of the pB construct adapted easily for both gain- and/or loss-of-function genetic screens (Chew SK, 2010). In conclusion, pB transposon vectors are an extremely versatile and powerful means for genome-wide mutagenesis in mammalian cells.

Transfetion of pB system (including pB vector and trasposase) in ES cells (Figure 2.A) resulted in random genome-wide integration leading to the generation of library of thousands of independent mutants where individual genes will be activated (step 1 of the screening strategy). After selection of mutants displaying the phenotype of interest (step 2), the next stages of the screening are the identification of mutated locus in each clone and validation that such phenotype is dependent on pB integration (phenotypic rescue of the mutant could be obtained by removing pB vector). Further independent experimental validations will follow to characterize and confirm the protective activity of novel candidate genes.

Aim

Huntington's disease (HD) is an incurable neurodegenerative disorder caused by CAG expansion in Htt locus leading to loss of striatal neurons. The main objective of my PhD thesis was to identify and characterize novel genes involved in HD. Combining mouse Embryonic Stem (ES) cell properties of ease of genetic manipulation and high genomic stability with piggyBac mediated-insertional mutagenesis, I performed a genetic screen for potential therapeutic targets for HD.

A preliminary screening for regulators of SRF pathway, advantaged by availability of a fluorescent reporter for SFR activity, was set up in order to acquire technical expertise required for the screening procedure.

Subsequently, I carried out gain-of-function screen on ES cell lines stably expressing mutant Htt (Q128 Htt) and succeeded in identification of a set of candidate genes that are able to reduce the toxic effects of mutant Htt. Such genes, after extensive validation *in vitro* and *in vivo*, will represent novel promising therapeutic targets for HD.

Results

In the introduction I described a general approach to perform genetic screening using ES cells (Figure 2.A). In order to set up the entire experimental system required to perform a genetic screening I first performed a screening for regulators of SRF signalling, taking advantage of an available fluorescent reporter for monitoring SFR activity (a kind gift from Prof. Dupont at Padua University). The use of such available reporter makes the screening procedure easier to perform, allowing me to focus on the optimization of the technical aspects of the entire procedure. Moreover, the SRF pathway is a key pathway of cell biology, linking mechanical stress to gene-expression and it is only partially defined, therefore identifying novel components and regulators of this pathway could be of interest. Finally, the SRF pathway has never been implicated in Huntington disease; given that any screening procedure can generate false positive hits, due to technical biases and artefacts, by performing two completely unrelated screenings I have been able to identify genuine targets and filter out false positives (see below).

The transcription factor SRF (Serum Response factor) specifically recognizes SRF Responsive Elements (SREs) found within the promoter region of target genes (such as Egr1 and Tagln). SRF has been involved in several biological processes, such as keratinocytes self-renewal and mesoderm differentiation.

SRF targets expression is rapidly induced either by serum or by mechanical stress via actin/Rho/MAL activation. Rho (a member of small GTPases family) regulates the assembly of polymerized actin (F-actin) and the ratio of F-actin to G-actin (unpolymerized actin) correlates with the level of SRF activation. A G-actin binding protein, known as MAL is a mediator of signals from Rho to SRF (Miralles F., 2003). MAL is predominantly localized in the cytoplasm, where it is sequestered by actin monomers. Upon serum stimulation (and Rho activation), F-actin accumulates in the cytoplasm and MAL can associate with SRF in order to activate a subset of SRE-containing genes (Vartiainen M.K., 2007). Mechanical signals have also been shown

to influence SRF activity (Connelly J.T., 2010), possibly via actin fibres, but the mechanism is still unknown. Similarly, it is not known what serum does on the cells leading to SRF activation (i.e. what are the receptors mediating serum response?).

Generation of SRF-GFP ES cells

It is easy to detect the activity of the SRF pathway by mean of a reporter construct containing a SRE, a minimal Promoter, both followed by GFP (Figure 3.A). Thus, GFP protein will be produced when the SRF pathway is active (Figure 3.A, right).

SRF-GFP ES lines were generated by electroporation of SRF reporter in E14 cells, a wild-type ES cell line commonly used for *in vitro* studies and generation of transgenic mice. The reporter has been introduced in ES cells by electroporation, resulting in random genomic integrations. Several clonal populations have been expanded and characterized. Each clonal line possesses different integration site, therefore the activity of the reporter could potentially differ in different lines. For this reason I characterized the reporter activity in several clonal lines and chose a single cell line showing the expected behaviour, called SRF-GFP ES cells (Figure 3.B). First (Figure 3.B, from left to right), I observed no basal activation in the absence of serum in the medium. Second, I observed rapid activation in presence of 15% serum. Third, I observed robust activation upon treatment with Cytochalasin D (CD) in the absence of serum. CD inhibits actin polymerization by binding with high affinity to growing ends of actin nuclei and filaments (F-actin) and preventing addition of monomers (G-actin) to these sites, thus MAL is free to translocate to the nucleus and promote SRF target gene expression (Figure 3.A, right). I conclude that the reporter responds correctly to both serum and cytoskeletal inputs. To further validate our experimental setup I tested whether reporter activation was dependent on SRF levels, and found that siRNA-mediated knockdown of SRF ablated the activity of the reporter measured by flow cytometry (Figure 3.C). I also looked at the endogenous SRF target Tagln and it was found induced by CD and downregulated after SRF knockdown (Figure 3.D).

I therefore concluded that our reporter system allows to faithfully monitor SRF activity and can be used to carry out a gain-of-function genetic screening.

Genome-wide screen for novel regulators of SRF signalling

As described in the introduction, the main steps of a genetic screening are:

1) generation of a library of mutant clones;
2) identification of clones displaying a phenotype of interest;
3) identification of the gene mutations conferring such phenotype;
4) further functional validations of individual genes.

In the case of the SRF screening I used the activation of the SRF-GFP reporter to identify the clones displaying a phenotype of interest. In order to generate our library of mutant clones, I decided to perform mutagenesis by electroporation of a piggyBac (pB) retrotransposon vector called pGG134 (Guo et al., 2010) on SRF-GFP ES cells. This construct (shown in Figure 4.A, see methods for details) integrated randomly into the genome, forcing the over-activation of nearby genes. DsRed and Hygromycin cassette are included and used to identify cells with successful pB vector integration, that will be DsRed positive and Hygromycin resistant.

I electroporated the pB system (including pGG134 vector and pBase) in SRF-GFP ES cells and generated a library of thousands of independent mutants, each one with different over-activated genes (a schematic representation of screening strategy used is shown in Figure 4.B). After Hygromycin selection for pB integration, I analysed cells by flow cytometry and found that >85% of cells were DsRed positive, indicating successful integration of the pGG134 vector (Figure 4.C, top left quadrant). Only a small fraction (~1%) of DsRed positive cells were also positive for the SRF-GFP reporter (red dots in P3 region). All these experiments were performed using serum-free media, therefore the activation of SRF-GFP reporter in such rare cells is likely due to over-expression of a gene involved in SRF signalling. Mutant double positive cells were collected by FACS (Fluorescence-Activated Cell Sorting) and expanded. By repeating this straightforward procedure (including electroporation, selection and cell sorting), a collection of hundreds of distinct mutant ES cell lines has been generated.

The rare double positive cells can be isolated and expanded as single independent lines. I generated 63 different clonal lines, each one carrying different activating mutations. The identification of the mutated gene of each individual clone will be obtained by Splinkerette PCR (Mikkers H, 2002), a technique allowing the amplification of genomic fragments flanking pB integration site. PCR products will be sequenced in order to identify the precise site of integration in each mutant line. In parallel, genome-wide analysis of the integration sites (Carette JE, 2010) on 4 entire populations of mutant clones will be performed by Next Generation Sequencing (NGS). By combining the two data sets, a list of genes involved in SRF signalling will be generated. Validation of candidate genes as novel regulators of SRF signalling will be finally performed.

Identification of over-activated genes in mutant clones

After isolation and expansion of double positive clones (Figure 4.C), the next step of our strategy is to identify the insertion site in each clone and then to verify that the mutation is responsible for activation of the SRF pathway. To this aim I performed Splinkerette PCR (Sp-PCR), which allowed amplifications of genomic fragments flanking the pB integration site (schematic overview of Sp-PCR product in Figure 5.A, see also Methods).

Genomic DNA of individual clones is digested with a restriction enzyme (BstYI) that cuts the frequent consensus sequence GATC. Adapters are ligated to all the resulting fragments of genomic DNA. PCR is then performed, using specific primers annealing to the pB vector and the adapters. This procedure is repeated for both the 5' and 3' end of the pB vector, to increase the chances of successful identification of the genomic integration site. Ideally, each mutagenic event was unique for single mutant clonal line and should be recognized by a single PCR band (for the pB5' and pB3' transposon/host junctions). The gel electrophoresis in Figure 5.B shows Sp-PCR products from several mutant clones, namely B10-B13. One or two major bands were clearly distinguishable for almost all the clones, which correspond to amplification for the 5' and/or 3' end of the pB vector, respectively.

Selected single PCR band (as the one highlighted in a red square in Figure 5.B) was then excised from gel, purified and sequenced with the same pB primers used for PCR. The sequence obtained includes a portion of genomic DNA (Figure 5.C, red) followed by BstYI restriction site (GATC sequence, black) and the sequence of adapter (blue). Finally, the genomic sequence was aligned to the reference genome, allowing identification of the precise site of integration in each mutant cell line: in the example shown in Figure 5.D, the pB vector was found inserted upstream of the Xbp1 gene and in the correct orientation allowing its activation.

I repeated Sp-PCR and analysis of PCR bands for all clones collected. Therefore, a list of candidate genes has been generated (Figure 5.E), including some transcription factors, transmembrane protein and kinases that are potential regulators of SRF activity.

In order to validate our methodology I randomly selected some clones (highlighted in blue in Figure 5.E) and check whether the reporter was still active and, more importantly, whether the endogenous SRF targets were upregulated. Flow cytometry analysis on selected mutants cultured in the absence of serum revealed that all clones were DsRed positive, indicating stable integration of the pB vector, and SRF reporter activation was maintained for prolonged culture (Figure 6.A). The endogenous SRF target gene Egr1 was rapidly induced by serum in parental SRF-GFP cells, and it resulted upregulated in the absence of serum in all 4 clones analysed (Figure 6.B). I conclude that the screening procedure allowed the generation of mutant clones displaying the phenotype of interest (stable activation of the SRF pathway) and to identify genes that could be putative novel regulators of this pathway.

In parallel, genome-wide analysis of the integration sites was performed by NGS after Sp-PCR on the entire population of mutant clones (Figure 4.B). This analysis independently confirmed the identification of 7 genes out of the 20 found in individual clones. Moreover I found several genes related to those identified in single clones (e.g. Mbln1 and Mbln2). In total 102 genes were identified as SRF regulators.

Not only this genome-wide analysis of SRF regulators has been instrumental to establish all the methods required for a genetic screening (electroporation, Sp-PCR etc), it will be also ground for future investigations. Moreover, I used results from the SRF screening to analyse similar data obtained in the Htt screen in order to identify genes specifically associated with the phenotype of interest and to filter out likely false positives that recurred in both screens, possibly due to hot spot sites of integration (see below).

Generation and characterization of Q128-Htt ES line.

Taking advantage of the methods developed thanks to the SRF screening I then set up the experimental system to perform a screening for regulators of toxicity caused by mHtt. Embryonic Stem (ES) cells expressing a N-terminal fragment of either mutant (such as the HttQ128 allele) or wild-type (HttQ15) Htt were obtained by DNA transfection and selection of clones with stable integration (see in methods details of HD plasmid used). This resulted in the generation of ES cells that stably express increased levels of either mutant or wild-type Htt mRNAs, named Q128 Htt and Q15 Htt, respectively (Figure 7.A). Correct production of mutant (80kDa) and wild type (65kDa) form of Htt protein in Q128 and Q15 cells was confirmed by Western Blot (Figure 7.B). Although Q15 and Q128 Htt ES lines showed both similar high expression level of Htt mRNA, they differed in Htt protein content: the mutant protein was expressed at considerably lower levels than wild-type Htt. This could be explained by reduced stability of Q128 Htt.

Despite the low levels of Q128 protein, compared to Q15, Q128 Htt cells showed a pronounced reduction in their number over time (Figure 7.C). Similar results were obtained from independent transfections of two different parental ES cell lines (data not shown). I conclude that expression of mHtt impaired viability of ES cells.

My aim is to perform a genome-wide screening to identify genes that are able to reduce cell toxicity caused by mHtt. In order to perform a genetic screening it is important to have a clear readout, such as the activation of a reporter gene, as in

the case of SRF-GFP, or simply the capacity of a cell to survive under specific experimental conditions.

Expression of mHtt impaired expansion of ES cells. It has been previously reported that exogenous stressors, such as autophagy or proteasome inhibitor, could exacerbate the toxic effects of mHtt (HD iPSC Consortium, 2012). Thus I reasoned that by treating our Q128 Htt cells with different cell stressors I could induce their death. Such experimental conditions would be ideal to perform a genetic screening, whereby rare mutants would survive, thanks to the activation of genes conferring resistance to mHtt (Figure 7.D).

Effect of selected cellular stressors on HD lines.

In order to identify cellular stressors that increase the toxic effect of mHtt I first screened the literature and found some biological processes implicated in HD (Zuccato C, 2010). Autophagy and the ubiquitin/proteasome system are known to mediate the degradation of abnormal protein products. Specifically in HD, both pathways could have a role in enhancing clearance of mHtt, i.e. the use of autophagy or proteasome inhibitors would result in mHtt accumulation in cellular compartments (Ju J-S, 2014; HD iPSC Consortium, 2012). I selected also other compounds that have been previously shown to exacerbate the toxic effects of mHtt, such as hydrogen peroxide (H_2O_2; Jonson, I 2013), Tamoxifen (Ellerby LM, 1999; Wellington CL, 2000) and Rotenone (inhibitor of complex I, mitochondrial respiratory chain).

I then selected a panel of inhibitors (Figure 8.A) and titrated them in parental ES cells to find doses that were not lethal after 48 hours of treatment (Figure 8.A, right column). I treated Q15 Htt and Q128 Htt cells with the inhibitors and quantified the number of surviving cells by Crystal Violet (CV) staining. I observed two different outcomes: in the case of Rotenone, or autophagy inhibitors (such as 3-Methyladenine, Bafilomycin A1 and Chloroquine), I measured a strong decrease in the number of cells, irrespectively of whether they expressed wild-type or mutant Htt (Figure 8.B, top panels). Conversely, treatment with the proteasome inhibitor MG132 or with Tamoxifen, affected Q128 Htt more than Q15 Htt cells (Figure 8.B, bottom panels). Therefore, MG132 and Tamoxifen were chosen as stressors

selectively inducing cell death in ES cells expressing mHtt, to be used for the genetic screening approach described in Figure 7.D.

I decided to use two independent stressors, acting on different biological processes, for the following reason: a screening performed only with, for instance, the proteasome inhibitor will very likely identify genes that rescue Htt effects by activating the proteasome. By performing the screening with two different stressors and taking candidate genes that display an effect regardless of the stressor used, I should identify candidates that specifically act on mHtt.

Screening strategy used to identify new proteins involved in Htt-dependent toxicity.

Electroporation of pB system (including pGG134 pB vector, shown in Figure 4.A, and transposase) in Q128 Htt ES cells resulted in the generation of thousands of independent mutants, each one with different over-activated genes (a schematic representation of screening strategy used is shown in Figure 9).

After Hygromycin selection for pB integration, cells will be exposed to lethal concentrations of selected exogenous stressors. ES cells bearing over-activation of a gene conferring resistance to effect of mHtt will survive and generate colonies that will be picked and expanded. By repeating this procedure, using different stressors, a collection of hundreds of distinct mutant ES cell line will be generated. The identification of the mutated gene of each individual clone will be obtained by Sp-PCR, as described above. Also in this case, genome-wide analysis of the integration sites on entire populations of mutant clones will be performed by NGS. Therefore, a list of genes conferring resistance to mHtt will be generated. Validation of candidate genes as “suppressors” of mHtt toxicity will be further performed.

Genome-wide screen for new genes conferring resistance to mutant Htt

To successfully perform a genetic screening I used the following controls:

1) parental ES cell line, that do not express mHtt, was electroporated with an

empty pB vector (EV) and underwent the entire screening procedure. Such cell line should survive;

2) Q128 Htt line electroporated with EV that should die after exposure to stressors.

The electroporation of the pGG134 vector in Q128 Htt cells should result in an increased number of clones, thanks to the survival of rare mutant colonies.

I generated the 3 indicated cell lines by electroporation, I selected with Hygromycin for 2 weeks to ensure stable pB integration, and finally exposed cells to exogenous stressors for other 5 days. Surviving colonies were stained for counting. Parental ES_EV cells, that expressed no mHtt, did not show cell death upon MG132 treatment (Figure 10.A, left). Very few Q128_EV mutant colonies survived to MG132 or Tamoxifen treatment, while Q128_pGG134 mutants were significantly more abundant in presence of both of stressors (Figure 10.A-C). I conclude that the increased number of surviving colonies in Q128_pGG134 was due to the mutagenesis procedure.

I collected a total of 17 populations of mutants emerged from different mutagenesis/selection cycles (Figure 10.D) with MG132 or Tamoxifen. Moreover, I individually picked and expanded a total of 44 clonal lines emerged from mutant populations generated.

Identification of the over-activated genes in mutant Htt-resistant clones.

The next step of our screening strategy (Figure 9) was the identification of the genes activated in individual clones by Sp-PCR, which allow amplification of for the pB5' and pB3' transposon/genomic junctions (Figure 5.A).

Ideally, each mutagenic event was unique for single mutant clonal line and were recognized by a single PCR band (for 5' and 3' end of the pB vector). The gel electrophoresis in Figure 11.A shows Sp-PCR products from several mutant clones, namely MG15-17. Two major bands are clearly distinguishable in the first and the second lane, which correspond to amplification for the pB5' and pB3' in clone

MG15 and in other 34 clones analysed. In contrast, multiple bands were detected in MG16, while no PCR bands in MG17. These outcomes are due to technical limitations of Sp-PCR that did not allow me to identify integration sites in 9 out of 44 clones analysed.

Selected single PCR band (highlighted in red square Figure 11.A) was then excised from gel, purified and sequenced with the same pB primers used for PCR. The sequence obtained includes a portion of genomic DNA (Figure 11.B, red) followed by BstYI restriction site (GATC sequence, black) and the sequence of adapter (blue). Finally, the genomic sequence was aligned to the reference genome, allowing identification of the precise site of integration in each mutant cell line: in the example shown in Figure 11.C, the pB vector was found inserted upstream of the Kdm5b gene and in the correct orientation allowing its activation. The integration of the pB vector in proximity of a given gene may indicate that such gene is over-activated. It is necessary to prove that the putative target gene is in fact more expressed in the clone under analysis compared to control ES cell lines. I measured expression level of Kdm5b gene by qPCR and it resulted upregulated in selected clone MG15 (Figure 11.D, top left), compared to both the parental and the Q128 Htt cell line. I conclude that the pB integration successfully resulted in activation of the Kdm5b gene in clone MG15.

I carried out the same analysis for the all the clones collected (named MG# or T#, according to their derivation from MG132 or Tamoxifen, respectively) and for most of them I was able to map the genomic integration site. I chose 6 candidates for further validations, focusing on the most reliable ones, in which a single PCR band for 5' and 3' end of the pB vector identified the same genomic integration site. In such clones I measured expression level of the gene identified by qPCR (Figure 11.D) relative to control ES cells and the Q128 cells transfected with an empty vector (Q128_EV). I confirmed upregulation of the candidate gene in the corresponding clone compared to control ES cells. Specifically, I proved upregulation of Qk gene in MG3 clone, Fbxo34 in MG21, and also (Figure 11.D, bottom) Mtf1 in MG18, Synj2 in MG9 and Arid1b for clone T4. Such results demonstrated that integration of pB on

target promoters resulted in upregulation of the cognate genes, that are therefore candidate targets conferring protection from mHtt toxicity.

Characterization of selected mutant clones

The next step is the characterization of the 6 clones for which I identified the over-activated target genes. The screening procedure selected rare mutants resistant to cell death induced by mHtt in the presence of stressors. Thus the clones should show the same phenotype. When exposed to both exogenous stressors individually, parental ES cells survived (Figure 12.A top: MG132, bottom: Tamoxifen treatment), Q128 Htt cells massively died, while all clones survived. Quantification of the number of surviving cells by Crystal Violet after 48hrs of treatments with MG132 or Tamoxifen is reported in Figure 12.B and 12.C. All lines were significantly more resistant than Q128 cells. The evidence that the clonal lines were resistant to both stressors suggest that the mutagenesis procedure led to activation of genes conferring resistance to mHtt, rather than resistance to MG132 treatment itself.

The fact that some clones acquired resistance could be due to the silencing of the Q128 transgene. To rule out such scenario, I measured the expression levels of HttQ128 mRNA and protein. By qPCR and Western Blot analyses (Figure 12.D and 12.E), I confirmed that mHtt was still present in selected clones, with variations of maximum 3 fold relative to Q128_EV controls. Therefore I conclude that the identified 6 target genes seems to confer resistance to mHtt without decreasing its expression levels.

Analyses of the pattern of integration of pB vectors in resistant clones

I repeated Sp-PCR and analysis of PCR bands for all clones collected. In 20% of clones the target genes could not be identified because no PCR bands or too many bands were detected, or no clear matches to reference genome were found (Figure 13.B, “unidentified”). In most of the cases (80%), I was able to identify the putative

target genes, that are listed in Figure 13.A. Bioinformatic analysis of the list of mutated genes was used to identify specific pathways, gene families or molecular complexes associated with suppression of mHtt toxicity (Figure 13.B). A large fraction (~30%) of genes included transcriptional regulators; nearly 10% of genes were members of Golgi-ER network. The remaining ~40% of genes were associated to diverse biological processes. I conclude that this approach allowed the identification of different classes of genes.

In parallel, genowe-wide analysis of the integration sites was performed by NGS after Sp-PCR on 17 entire populations of mutant clones. The elevated number of populations analysed allowed identification of >400 genes from both the MG132 and the Tamoxifen treated populations. I reasoned that genes identified under both conditions are more likely to be direct regulators of mHtt cellular stress. Different mutagenesis strategies (e.g. retroviral vectors, retrotrasposon vectors, gene-trap vectors) can generate false positive hits due to genomic sites where integration is favoured (hotspots of integrations). I performed genome-wide screening also for SRF regulators, a biological process completely unrelated to mHtt toxicity. Direct comparison of the screening results indicated that 56 genes were identified in all screenings (Figure 13.C), suggesting that such integration sites are hotspots of integration and therefore were discarded from further analyses. Of note, one of such genes was Qk that was also identified in several individual clones (Figure 13.A), confirming that it represents a hot spot integration site; therefore it was excluded from further validation experiments.

154 genes were confirmed as *bonafide* suppressors of mHtt cell stress. Bioinformatic analysis of such genes confirmed enrichment for transcriptional regulators (as resulted for Sp-PCR gene list Figure 13.B). More than 20% of the genes were epigenetic modifiers or transcription factors; minor fractions (7% and 4%) of gene were involved in proteasome degradation or vescicular trafficking (respectively). The remaining ~60% of genes could not be linked to a common specific pathway (Figure 13.D).

The over-representation of transcriptional regulators I observed both in individual clones and in entire populations is consistent with several reports showing that

mHtt causes deregulation in transcriptional activity (Benn CL, 2008). Moreover, among the 154 genes I found either the same 6 genes upregulated in the clones under analysis, or very closely related members of the same protein family (e.g. Kdm1b, Kdm2b, Kdm4c and Kdm5b or Mtf1 and Mtf2). In sum, identification of target genes either by Sp-PCR of individual clones, or on entire populations by NGS gave consistent results and allow to exclude hotspots of integration.

Validation of candidate genes as "suppressors" of mutant Htt toxicity

The 6 clones I isolated are resistant to Q128 Htt and cell stressors (Figure 12.A-C). If such resistance is conferred by the activation of cognate genes by the pB vector, I expect that upon excision of the pB vector the clone will become again sensitive to stressors in presence of mHtt.

In details, LoxP sites are located near the 5' and 3' end of pGG134 vector (Figure 14.A and methods), allowing efficient and precise excision of the vector content from the genome of mutant clones. Transfection of the CRE recombinase should result in removal of the entire pB vector, including DsRed and Hygromycin resistance gene (Figure 14.B). So it is possible to monitor the efficiency of excision by exposing clone to Hygromycin selection, or by measuring the levels of DsRed expression by flow cytometry.

For this functional validation I excluded the clone MG3 given that Qk represented a hot spot of integration. I transfected all the other 5 clones with CRE recombinase and observed loss of resistance to Hygromycin (not shown) and decreased DsRed signal for all mutant clones. Unfortunately the clone MG18/Mtf1 was lost during the procedure after a bacterial contamination.

Representative flow cytometry profiles for clones MG15 and MG9 were shown in Figure 14.C: both clonal line MG15 and MG9, showed decreased DsRed signal upon CRE transfection (Figure 14.C, right panels). Their un-transfected counterpart retained resistance to Hygromycin selection and were homogeneously DsRed positive (Figure 14.C, middle).

The percentage of DsRed positive population quantified for all mutant clones before and after pB excision is reported in Figure 14.D. Wild-type and Q128 Htt ES cells were included as negative controls; ES cells transfected with a vector containing a constitutive DsRed cassette (ES wt_EV) were used as positive controls and were >92% DsRed positive. I concluded that transient Cre transfection resulted in complete removal of the pB cassette.

I then tested whether excision of the pB vector resulted in increased sensitivity to cell stressors. To address this, I exposed cells to MG132 or Tamoxifen. As expected, clones confirmed increased resistance to MG132 and Tamoxifen treatments compared to Q128 Htt cells (Figure 15.A and 15.B, compare bars 3, 5, 7 and 9 vs 2), measured by number of surviving colonies stained after 48hrs of treatments. Interestingly, for clones MG15 and T4 I observed a significant decrease in cell survival after Cre-mediated excision (compare bars 6-5, and 10-9). These results confirmed that the phenotype previously observed on clones was due to the pB integration. The fact that also after excision cell viability was still more pronounced in the mutant clonal lines than in control ES cells, indicated that some additional compensatory mechanisms occurred during extended culture *in vitro*.
In contrast, transfection of CRE in clone MG9 or MG21 did not decrease the capacity of mutant cells to expand in both stress conditions (Figure 15.A and 15.B). I conclude that the MG9 and MG21 clones showed increased resistance independently from the pB vector integration, suggesting the presence of some artefactual compensatory mechanism independent from the mutagenesis procedure.

To exclude possibility that the increased proliferation ability of clones might be due to alterations in mHtt expression, I performed Western Blot analyses for HTT protein (Figure 15.C) and confirmed that mHtt was detectable in all the selected clones at the same or higher levels compared to Q128_EV cells. Thus clones displayed increased survival without affecting the expression levels of HttQ128.
Overall this set of experiments allowed identifying the two clones MG15/Kdm5b and T4/Arid1b where the increased survival was due to integration of the pB vector.

Moreover, this set of experiments clearly showed that also some artefactual events, possibly due to extended culture, could lead to increased resistance independently of the mutagenesis strategy. Being aware of such effects is crucial and requires further independent validations to identify genes that confer resistance to mHtt.

Independent validation of candidates as genes conferring resistance to Q128 cells

To further confirm that our candidate genes are able to confirm resistance to mHtt I performed an experiment (depicted in Figure 16.A) whereby Q128 cells are transfected with a vector containing cDNA of candidate genes under the control of a constitutive CAG promoter (Q128_candidate), or an empty vector that served as control (Q128_EV). This is to rule out any artefact potentially caused by the mutagenesis strategy.

For this further validation we chose Kdm5b that showed pB vector-dependent effects, Fbxo34 that appeared as a false positive hit of our screening, given that the clone MG21 displayed resistance also after excision of the pB vector. In this sense Fbxo34 served as a negative control. Moreover, we included Mtf1 that showed protection in the first set of experiments (Figure 12) but could not be validated in the context of pB vector excision for technical reasons. Finally, I have not tested Arid1b yet because its cDNA is ~7kb long and proved hard to clone into an expression vector.

Firstly, I performed qPCR and Western Blot analyses (Figure 16.B and 16.C) to measure levels of HttQ128 mRNA and protein and prove that mHtt was properly expressed and produced in all the new cell lines generated. Secondly, I checked whether the expression of Mtf1, Kdm5b and Fbxo34 was indeed increased in Q128_Mtf1, Q128_Kdm5b and Q128_Fbxo cells, respectively, and observed high levels of expression in all cell line generated relative to relevant controls (Figure 16.D).

Finally, I checked whether the proliferation of Q128 expressing cells was affected by

co-expression of our candidates. Q128_EV cells displayed reduced proliferation relative to control Q15 cells (Figure 16.E) as expected from our initial characterization (Figure 7.C). Expression of Fbxo34 had no effect, while Mtf1 and Kdm5b led to increased proliferation.

I then exposed cells to stressors MG132 or Tamoxifen, and the vehicles DMSO or ethanol (EtOH), to test if expression of candidate gene conferred increased resistance to mutant Htt. Cells were plated under the indicated conditions and after 48h surviving cells were stained and quantified. I observed, as expected, a reduction in the number of cells in Q128_EV compared to Q15 cells already in the presence of the vehicles DMSO and EtOH (Figure 17.A and 17.B, left panels). Treatment with the stressors caused a severe reduction specifically of Q128_EV cells, relative to Q15 (right panels). Expression of Fbxo34 had a mild protective effect that did not reach statistical significance. In contrast, expression of Mtf1 and Kdm5b conferred resistance to stressors in Q128 cells.

I conclude that expression of Mtf1 and Kdm5b gene conferred resistance to mutant Htt, confirming the phenotype observed in the clones in which such genes were found upregulated. Overall these results indicate that Mtf1 and Kdm5b are indeed able to confer resistance to mHtt.

Discussion

I have described here a full methodology to perform a gain-of-function screening wih ES cells, that I used to obtain an understanding of the molecular mechanism of action of mutant Htt protein. Differently from conventional screenings for HD, the approach I developed is based on the use of mammalian (mouse) ES cell system and takes advantage of state of the art technology of piggyBac vector for achieving random genome-wide mutagenesis.

To set up all the techniques required for the screening procedure, I first carried out a preliminary gain-of-function screening for regulators of SRF signalling, a critical sensor of serum and mechanical forces in the cell. It could be of interest to identify novel components and regulators of an important pathway of cell biology, still not faithfully defined. But also, the use of a clear readout, such as the activation of SRF-GFP reporter, facilitated the screening, allowing me to optimize all the technical aspects of the entire procedure.

Firstly, I generated ES cell stably expressing a fluorescent reporter for monitoring SFR activity; then I performed pGG134-mediated mutagenesis and enrichment by sorting of mutant population showing stable activation of SRF-GFP reporter upon pB integration. Importantly, also endogenous SRF targets were activated together with the SRF-GFP reporter in individual clones. For each clone the activated locus was identified by Sp-PCR, therefore I found some promising targets as stable “activators” of the SRF pathway. Moreover, Next Generation Sequencing analysis of entire populations of mutants was carried out, allowing identification of 102 potential SRF regulators. In addition to giving novel insights on how SRF is regulated, such data have been used for direct comparison of similar results obtained from a completely unrelated screenings (for regulators of HD toxicity) allowing to recognize genuine targets from false positive hits (see below).

The screening for HD was also based on the pGG134-mediated mutagenesis with the aim of identifying candidate "suppressors" of mHtt toxicity. To do so, I generated ES cells stably expressing mutant (Q128) Htt, characterized them and observed impaired proliferation and increased sensitivity to MG132 and Tamoxifen stressors. I performed mutagenesis on Q128 Htt cells and screened for rare clones surviving to mHtt toxicity thanks to over-activation of some genes. By Sp-PCR I identified pB integration sites for 80% of mutant clones analysed and found a set of candidate genes that are potentially able to reduce the toxic effects of mHtt. I distinguished different classes of genes, including member of Golgi-ER network, proteasome degradation complex or vescicular trafficking. Notably, the most enriched class of genes was transcriptional regulators. This was consistent to evidence that one of the cellular alterations caused by mHtt regarded transcriptional activity and chromatin regulation (Sugars KL and Rubinsztein DC, 2003; Benn CL, 2008; Biagioli M, 2015).

From a list of 154 genes identified, we prioritised 6 genes for further validation.

The selection criteria adopted were:

1) Recurrence of the target in both NGS-population analysis and individual clones by Sp-PCR;

2) Identification of similar genes or members of the same gene family or biological pathway (e.g. Kdm1b, Kdm2b, Kdm4c and Kdm5b, or Mtf1 and Mtf2).

After extensive validation, consisting of a phenotypic rescue experiment in mutant clones (loss of resistance to mHtt toxicity upon pB excision by CRE recombinase) and overexpression of candidate in Q128 Htt ES cells (to confirm survival capacity in MG132/Tamoxifen) 3 genes were confirmed and all of them were transcriptional regulators.

Kdm5b (Lysine-specific demethylase 5b) protein is responsible of demethylating tri-, di- and monomethylated lysine 4 of histone H3, acting as transcriptional repressor. There is no previous evidence of a causal link between Kdm5b (or similar genes) to HD. I observed increased resistance to mHtt upon Kdm5b upregulation, future experiment will help identifying the mechanism of action. Of note, KDM proteins could also act as demethylases of other substrates, such as huntingtin protein itself, in line with recent reports showing that another polyQ containing protein, Androgen receptor, is indeed regulated by methylation (Scaramuzzino C, 2015).

Mtf1 (Metal-Responsive Transcription Factor) is a transcription factor that specifically binds MRE (metal response element) and promotes transcription of metallothionein genes upon exposure to heavy metal or other stressful conditions, as oxidative stress or infection. Saini et collegues reported that in *parkin* mutant flies the combined loss of Parkin and Mtf1 is synthetic lethal because of the increased ROS production, while the overexpression of Mtf1 or Mtna (Metallothionein A) gene rescued *parkin* mutant phenotype acting as antioxidants (Saini N, 2011). Mutant Htt has been shown to increase susceptibility to oxidative stress because of mitochondrial dysfunction (Zuccato C, 2010), thus it is easy to speculate that the protective effect of Mtf1 could be due to reduced oxidative stress in cells expressing mHtt.

The third candidate Arid1b (AT-Rich Interaction Domain 1B) was partially validated, due to technical limitations, as cloning its ~7kb long cDNA has proven hard. Arid1b is a component of the SWI/SNF chromatin remodeling complex, mediating, for example, differentiation of neural progenitor stem cells to post-mitotic neurons. In addition to gene regulation activity, it has a role in cell-cycle activation by mediating expression of c-Myc (Nagl, N .2007). To date, Arid1b has not being implicated in neurodegenerative diseases, but it has been recently reported that haploinsufficiency of Arid1b leads to altered brain gene-expression and autism-related behaviours (Shibutani H, 2017).

In addition to discussing the candidates that were successfully validated, it is equally important to describe the technical limitations of the genetic screening I carried out.

Of the 6 candidates I validated 50% were discarded for the following reasons:

1) Hotspot of integrations: when I compared NGS data from two completely unrelated screenings (SRF versus HD) 56 genes were identified in both, suggesting that such integration sites are hotspots of integration. Of note, Qk gene was initially identified as the most promising candidate in the HD screening, given its recurrence in several individual clones, but comparative analysis of NGS data confirmed that it was an integration hotspot; therefore it was excluded from further validation experiments.

2) Among all the clones in analysis, false positives are also expected, as some resistant Q128_EV colonies survived to MG132 or Tamoxifen treatment in several rounds of mutagenesis (Figure 10.B and C). Such cells acquired resistance to mutant huntingtin independently from the mutagenesis procedure. For instance, the MG9/Synj2 or

MG21/Fbxo34 clones did not show reduced resistance in presence of MG132 or Tamoxifen upon pB excision, meaning that the phenotype was not dependent on integration of the PGG134 vector, but rather to some adaptation mechanisms.

Of note, when Q128 Htt cells were extensively kept in culture I often observed a reduction in the cytotoxic effect of mHtt, suggesting that compensatory mechanisms occurred. The simplest hypothesis would be the inactivation of the Q128 transgene. For this reason in all validation experiments I have always checked mRNA and protein levels of Q128 and I found them unchanged. I conclude that other unknown mechanisms are in place to confer adaptation to mHtt.

Moreover, for several clones I was not able to identify univocally the activated gene conferring resistance to mHtt, because of the following technical limitations of Sp-PCR and pB-mediated random mutagenesis:

a) no Sp-PCR bands were detected in some clones;
b) no optimal Sanger sequencing results because of repetitive elements did not generate clear matches on the reference genome;
c) multiple integrations made difficult to identify the gene conferring resistance;
d) integrations occuring at more than 20kb upstream or downstream of the Transcription Start Site (TSS) also made difficult to identify the gene conferring resistance.

Overall, with this work I demonstrated the feasibility of a genome-wide screening in a mES cell model of a neurodegenerative disease. Several other candidates will be validated in the future, first in ES cells and then in more relevant model systems, such as immortalized striatal neurons expressing mHtt and animal models. To this aims I already established a Zebrafish model of mHtt in collaboration with Prof. Moro at the Department of Molecular Medicine at Padua University. The use of independent model systems will allow to gain insights into the biological mechanism linking over-activation of the target identified and reduced mHtt toxicity. Such genes, after extensive validation *in vitro* and *in vivo*, will represent novel therapeutic targets for HD. Most successful candidates could be addressed in HD patients by adeno-associated viral vector (AAV) for clinical gene therapy.

It will be interesting to test the role of the validated candidates in other diseases caused by expansion of poly-Glutamine tracts, such as spinocerebellar ataxias (SCA)

and spinobulbar muscular atrophy (SBMA). It is tempting to speculate that similar forms of cellular toxicity underlie all these pathologies.

Methods

Embryonic stem cell culture

Mouse embryonic stem (ES) cell lines used E14-Tg2a and Rex1GFP, derived both from 129 mice. ES cells were cultured in a humidified incubator at 37°C, 20% O_2 and 5% CO_2, in feeder free conditions (plastic coated with 0.2% gelatine [Sigma, cat. G1890]) and replated every 3–4 days at a split ratio of 1:10 following dissociation with either 0.25% Trypsin (Life Technologies) or Accutase (GE Healthcare, cat. L11-007).

Cells were cultured either in serum-free N2B27- based medium (DMEM/F12 and Neurobasal in 1:1 ratio, 0.1mM 2-mercaptoethanol, 2mM L-glutamine, 1:200 N2 and 1:100 B27 [all reagents from Life Technologies]) or serum–containing KSR medium (GMEM [Sigma, cat. G5154] supplemented with 10% KSR [Life Technologies], 2%FBS [Sigma, cat. F7524], 100mM 2-mercaptoethanol [Sigma, cat. M7522], 1× MEM non-essential amino acids [Invitrogen, cat. 1140-036], 2mM L-glutamine, 1mM sodium pyruvate [both from Invitrogen]), supplemented with two small-molecule inhibitors (2i) PD (1µM, PD0325901), CH (3mM, CHIR99021) from Axon (cat. 1386 and 1408) and LIF (100 units/ml produced in house), and 100 units/ml LIF.

Reverse transfection of ES cells

For DNA transfection, I used Lipofectamine 2000 (Life Technologies) and performed reverse transfection. For one well of a 6-well plate (9.4cm^2), we used 6µl of transfection reagent, 2µg of plasmid DNA and 300,000 cells in 2ml of medium. The medium was changed after overnight incubation.

Short interfering RNAs (siRNAs) were transfected at a final concentration of 40nM using RNAiMAX (Life Technologies), following the protocol for reverse transfection. For one well of a 12 well plate (4.9cm^2) we used 2µl of transfection reagent, 2µl of 20µM siRNA solution and 30,000 ES cells in 1ml of medium. The medium was changed after overnight (o/n) incubation; 48h after transfection the cells were analysed.

Electroporation of ES cells

I used electroporation method for:

a) stable ES cell line generation;

b) pB-mediated mutagenesis for genome-wide screening (discussed below).

In general, DNA linearization is required to improve efficiency of stable genome integration. In the case of piggyBac vectors such step is not required.

Electroporation protocol was performed as follows for both the cases:

1) 10cm dish of ES cells at approximately 80% confluency was harvested and resuspended in an appropriate volume of PBS, to a density of 1.0 x 10^7 cells/ml.

2) For each electroporation, 10^7 cells and 20-25µg DNA were mixed,

3) DNA/cell mixture was placed into a electroporation cuvette (Biorad Gene Pulser Cuvette, ca. 165-2088), avoiding to touch the metal plates.

4) Cells were electroporated by placing the cuvette in the electroporation holder of the Biorad GenePulser (ca. 165-2076). Settings used: 250V, 500µF, time constant should be between 5.6 and 7.5.

5) Electroporated cells were gently recovered from the cuvettes and plated.

6) Appropriate selection (Table 1 for antibiotics) started 24h after electroporation.

Electroporation of pB system on ES cells

For the screening procedure, careful titration of the amount of pB (vector and transpose) plasmids is fundamental to control the copy number. A single copy for cell is important to facilitate identification of the insertion site and therefore of the gene causing the phenotype of interest. I optimized condition to achieve a low number of integration events, by adjusting the ratio of pB vector vs transposase. I used a pB vector harbouring a DsRed reporter to monitore DsRed level by flow cytometry analysis (see below), so that the number of pB integration events would be proportional to the DsRed reporter signal. I electroporated ES cells with 2, 1 or 0.5µg of pB-DsRed vector, while keeping constant the amount of pBase-transposase (see Table 2). Almost 40% of DsRed positive cells resulted from electroporation of 10:1 of pBase:pB vector (combination A), while less than 30% were obtained by reducing amount of pB vector up to 1 or 0.5µg (combination B or C). No positive cells were

detected in wild-type ES cells, used as control cells. I concluded that lower amount of pB vector correlates with a lower number of integration events. For the screening strategy used in this work, mutagenesis was performed using the optimized amount of 0.5µg pB vector and 20µg pBase.

The pB pGG134 vector I used for mutagenesis procedure (shown in Figure 4.A) was optimized for gain-of-function screens (Guo et al., 2010): it consists of the murine stem cell virus (MSCV) enhancer/promoter followed by a splice donor (SD) site (in pink), which allows the over-activation of nearby genes. The pB 5'TR has also weak directional promoter activity, i.e. this construct can activate genes in either orientation. The vector contains also a second cassette, including a constitutive promoter followed by DsRed and Hygromycin resistance gene (in green). Thus cells that stably integrated the pGG134 vector will be DsRed positive and Hygromycin resistant.

Generation and characterization of SRF-GFP ES cells

SRF-GFP ES lines were generated by electroporation of SRF reporter in E14 cells, following electroporation protocol described above. A large-scale, overnight linearization of plasmid DNA was performed with the restriction enzyme EcoRI.

SRF reporter construct consists of a SRE, a minimal Promoter, both followed by GFP. A second cassette including Puromycin resistance gene under the control of a constitutive promoter, is used for selection of cells with stable integration. SRF-GFP ES cells were cultured in serum-free N2B27 2iL medium.

For reporter activation test, SRF-GFP ES cells were treated for 24h in serum 15% (GMEM [Sigma, cat. G5154] supplemented with 15% FBS [Sigma, cat. F7524], 100mM 2-mercaptoethanol [Sigma, cat. M7522], 1× MEM non-essential amino acids [Invitrogen, cat. 1140-036], 2mM L-glutamine, 1mM sodium pyruvate [both from Invitrogen]), or with of 2µM Cytochalasin D for 8h. Samples were analyzed by flow cytometry using a BD FACSCanto^{TM} cytometer.

For reporter inactivation experiment, two siRNAs targeting SRF (siSRF1 and SRF2) and a control siRNA were transfected on SRF-GFP ES cells cultured in serum-free N2B27 2iL

with of 2µM Cytochalasin D for 8h. Samples were analyzed by flow cytometry 48h after transfection.

Generation of HD lines

Q15- and Q128-Htt ES cells were originated from Rex1GFP ES cells by DNA transfection of vectors containing exon 1 of the huntingtin gene, with 128 or 15 CAG repeats respectively. Overnight linearization of plasmid DNA was performed with the restriction enzyme PvuI. Selection for transgenes was applied for selection of cells with stable integration.

HD ES cells were cultured in KSR 2iL medium.

Proliferation assay

Cell proliferation was assessed by plating 15,000 ES cells in 24-well plate (7,500 cells/cm^2) in presence of Puromycin 6µg/ml. Cells were counted every 24h for 4 days.

For stressors titrations (Figure 8, see Table 3), cells were plated in the presence of the inhibitors (and Puromycin 6µg/ml) for 48h and scored by quantification of the number of surviving cells by Crystal Violet (CV) staining. I treated Q15 Htt and Q128 Htt cells with the inhibitors and quantified the number of surviving cells by Crystal Violet (CV) staining (CV solution: 0.05% w/v Crystal Violet [Sigma], 1% of formaldehyde solution 37% [Sigma], 1% methanol, 10% PBS).

For pB-mutagenesis followed by stressor treatments, cells were plated at density 2,500 cells/cm^2 in Puromycin 6µg/ml and selected for 5 days in MG132 or Tamoxifen (Figure 10).

Response to stressors (MG132 or Tamoxifen in Figure 12, 15 and 17) was assessed by plating 5,000 ES cells in 24-well plate (2,500 cells/cm^2) in presence of Puromycin 6µg/ml. Surviving cells were stained by CV after 48h.

CRE-mediated pB excision

Mutant clones were kept in culture in presence of Hygromycin (Figure 4.A, details of pGG134 pB vector). Upon pB excision, Hygromycin resistance would be lost. So far, for this experiment Hygromycin selection was no more included in culture medium.
For pB excision, I used a Tamoxifen-inducible CRE recombinase construct (CRE), including Zeomycin resistance gene. Each clone was transfected also with an empty vector (EV), that underwent the entire protocol and died in presence of Zeomycin.
Transfection of CRE was performed following the protocol for reverse transfection. Zeomycin (Table 1) selection started 24h after transfection (day2). At day 3 Tamoxifen (800nM) was added for a total of 48h. Then, CRE-transfected clones and their un-transfected counterpart were compared by flow cytometry.

Flow cytometry

After enzymatic dissociation, ESCs were resuspended in PBS. Flow cytometry analyses were performed using a cytometer BD FACSCanto™ with BD FACSDiva™ software (Becton Dickinson). For cell sorting, ESCs were resuspended and collected in cell culture medium supplemented with penicillin-streptomycin (Life Technologies). FACS was performed using S3e™ Cell Sorter (Biorad).

Genomic DNA extraction and Splinkerette PCR

Cells were harvested and incubate o/n at 56°C with lysis buffer (10 mM Tris, pH 7.5; 10 mM EDTA; 10 mM NaCl; 0.5% w/v Sarcosyl, supplemented with proteinase K [Sigma cat #P2308] to a final concentration of 1 mg/ml). In order to obtain DNA precipitates, the next day 2ml of a mixture of NaCl and ethanol (30 ul of 5M NaCl mixed with 20 ml of cold absolute ethanol) was added. Cellular extracts were centrifuged for 45min at 4°C to remove soluble fraction. Precipitates (including gDNA) were rinsed three times by dripping 2ml of 70% ethanol and finally resuspended in 70°C-milliQ water.

A schematic overview of Sp-PCR procedure for pB-integration mapping (adapted from Potter and Luo, 2010) is shown below.

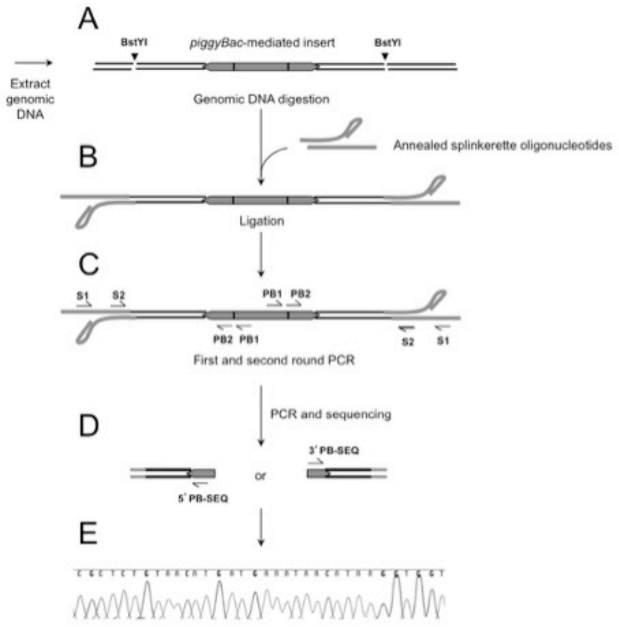

Sp-PCR protocol was performed as follows:

A) 2µg of genomic DNA were digested with 10U BstYI (10,000 U/ml) in a volume of 30µl. Reaction was incubated at 60°C o/n, the following day the enzyme was inactivated at 80°C for 20min.

Sp-adapters were generated by annealing of 150pmol of AdapterA and B primers (see Table 4) in a final volume of 100µl (10X NEB Buffer 2). Oligos were denatured at 65 °C for 5min, then cooled.

B) Ligation was performed in a total volume of 6µl including a 2X Ligation mix (Takara), 2.5µl of digested gDNA and 0.5µl Sp-adapters annealed. Ligation reaction was incubate at 16°C o/n, the next day 65°C for 10min for enzyme inactivation.

A purification step was included before step C, using QIaquick PCR Purification Kit, following manufacturer's instructions.

For PCR amplifications I used Phusion HF DNA Pol (NEB) in 5x Phusion GC Buffer recommended in case GC-rich templates or those with secondary structures. PCR mix included 5X GC Buffer, 10mM dNTPs, dmso and Phusion Pol.

C) First round PCR was amplified with 15µl of ligated DNA (or 50% of ligation product for each reaction for pB5' and pB3' transposon/host junctions), 0.5µM for each primer (Adapter-PCR1 and pB5' or pB3'-ITR PCR1), 6.5µl PCR mix, final volume of 25µl.

Sp-PCR1 program: 95 °C for 2min; two cycles of 95°C for 20sec, 65°C for 30sec, 68°C for 2min; then 30 cycles of 95°C for 30sec, 60°C for 30sec, 68°C for 2min; then 68°C for 10min.

PCR1 products were detected as DNA smear on a 1% agarose gel.

D) For second round PCR, I used 5µl of 1:500 dilution of PCR1 product, 0.5µM for each primer (Adapter-PCR2 and pB5' or pB3'-ITR PCR2), 6.5µl PCR mix, final volume of 25µl.

Sp-PCR2 program: 95 °C for 2min; two cycles of 95°C for 20sec, 65°C for 30sec, 68°C for 2min; then 5 cycles of 95°C for 30sec, 60°C for 30sec, 68°C for 2min; then 25 cycles of 95°C for 30sec, 58°C for 30sec, 68°C for 2min; then 68°C for 10min.

PCR2 products were analyzed on a 2.5% agarose gel: if the product was unique it can be sequenced directly; in case of multiple products, the major bands were excised and purified using a commercially kit prior to sequencing.

E) After treatment using Antarctic Phosphatase and Exonuclease I (both from NEB), PCR2 products were sequenced using pB5' or pB3'-ITR PCR2 primers.

Next Generation Sequencing analysis of genomic integration sites

Genomic DNA from entire populations of mutants was extracted using a Gentra Puregene Cell Kit. Library preparation and sequencing were performed by a collaborator (Dr. Martin Leeb at University of Vienna). Briefly, the first steps of Sp-PCR were performed on gDNA from populations of mutants. The second round of PCR was perfomed with Illumina compatible adapters, allowing Next Generation Sequencing of all PCR products. A bespoke bioinformatics pipeline allowed to map each single read to a genomic locus and to associate each site of integration to a gene within 20kb of distance.

Rna isolation, reverse transcription and quantitative PCR

Total RNA was isolated using RNeasy kit (QIAGEN), following manufacturer's instructions. Complementary DNA (cDNA) was made from 1µg of RNA using M-MLV Reverse Transcriptase (Invitrogen) and oligodT_{18} (500 µg/ml) primers. cDNA synthetized was quantified by Nanodrop ND-1000.

For real-time PCR, we used SYBR Green Master mix (Bioline. Cat. BIO-94020). Technical replicates were carried out for all quantitative PCR. An endogenous control (mGapdh) was used to normalize expression. Primers are detailed in Table 5.

Protein extraction and Wester Blot

Cells were washed in PBS and harvested with lysis buffer (50mM Hepes pH 7.8, 200mM NaCl, 5mM EDTA, 1% NP40, 5% glycerol). In order to obtain protein lysates, extracts were exposed to ultrasound in a sonicator (Diagenode Bioruptor). Cellular extracts were centrifuged for 10 minutes at 4°C to remove the insoluble fraction and total protein content was determined by Bradford quantification, preparing a calibration line using different BSA concentrations. Samples were boiled at 95°C for 5 minutes in 1X Sample Buffer (50mM Tris HCl pH 6.8, 2% SDS, 0.1% Bromophenol Blue, 10% glycerol, 2% 2-mercaptoethanol).

Each sample was loaded in a commercial 4-12% Nupage MOPS acrylamide gel (Life Technologies; BG04125BOX) and electrophoretically transferred on a PVDF membrane (Millipore; IPFL00010) in a Transfer solution (50mM Tris, 40mM glycine, 20% methanol, 0.04% SDS). Membranes were then saturated with 5% Non-Fat Dry Milk powder (BioRad; 170-6405-MSDS) in TBSt (8g NaCl, 2.4g Tris, 0.1% Tween20/liter, pH 7.5) for 1 hour at RT and incubated overnight at 4 °C with the primary antibody (see table 6). Membranes were then incubated with secondary antibodies conjugated with a peroxidase, diluted in 1% milk in TBSt. Pico SuperSignal West chemiluminescent reagent (Thermo Scientific; 34078) was used to incubate membranes and chemiluminescence from the interaction between peroxidase and substrate present in the commercial reagent was digitally acquired by ImageQuant LAS 4000.

Table 1. Antibiotics

Antibiotic	Cf
Puromycin	0.5-1 µg/ml
Hygromycin	150 µg/ml
Zeomycin	150 µg/ml

Table 2. Titration of pBase:pB vector ratio

Trasposon DNA amount (µg)			% DsRed positive
combo	pBase	pB vector	
A	20	2	36,9
B	20	1	28,3
C	20	0,5	28,2

Table 3. Panel of cellular stressors tested

Compound	Cat N	Diluted in	Dose range
Hydrogen peroxide	Sigma 216763	dd water	12.5-25 uM
MG132	Sigma M8699	dmso	12.5-25 nM
3-methyladenine	Sigma M9281	dd water	4-11 uM
Chloroquine	Sigma C6628	dd water	2.5-5 mM
Bafilomycin A1	Sigma B1793	dmso	6,25-12,5 uM
Rotenone	Sigma R8875	dmso	1-10 nM
Tamoxifen	Sigma T5648	etoh 70%	100-200 nM

Table 4. Splinkerette PCR primers

Sp-adaptor primer	Sequence
AdapterA hairpin strand with 5'-GATC overhang	GATCCCACTAGTGTCGACACCAGTCTC TAATTTTTTTTTTCAAAAAAA
AdapterB linear strand	CGAAGAGTAACCGTTGCTAGGAGAGACCGTGGC TGAATGAGACTGGTGTCGACACTAGTGG
Adapter PCR1	CGAAGAGTAACCGTTGCTAG GAGAGACC
Adapter PCR2	GTGGCTGAATGAGACTGGTGTCGAC
piggyBac primers	**Sequence**
pB3'-ITR PCR1	CAGTGACACTTACCGCATTGACAAGCACGC
pB5'-ITR PCR1	CCTCGATATACAGACCGATAAAACACATGC
pB3'-ITR PCR2	GAGAGAGCAATATTTCAAGAATGCATGCGT
pB5'-ITR PCR2	ACGCATGATTATCTTTAACGTACGTCACAA

ITR, piggyBac inverted terminal repeats

Table 5. PCR primers

Gene	Forward primer sequence	Reverse primer sequence
mTagln	AAGCCTTCTCTGCCTCAACA	CCTCCAGCTCCTCGTCATAC
mEgr1	CCCTATGAGCACCTGACCAC	TCGTTTGGCTGGGATAACTC
mGapdh	ATCCTGCACCACCAACTGCT	GGGCCATCCACAGTCTTCTG
mHtt	TGATGGATTCTAATCTTCCAAGG	GTGAGCCAGCTCAGCAAAC
mFbxo34	CCTCCCAGTCTTGAGTCAGC	CATAGGCGTTCTCAGGGTGT
mKdm5b	ACCTGACCTCCGACACAAAG	TGGCTTCTGTTGCCTCTTCT
mQk	GGAGCAAAATAGAGGCAAGC	CAGAATTGCAAGCTCCATCA
mMtf1	GAAGCAATGTCCCAGGGTTA	CTCCTCGGTGAGTCTTCTGG
mArid1b	CTGGACCTGTTCCGACTGTA	CAACGTTCAGGTTGGTTGC
mSynj2	CAGGAGGCAGAAGCAGCTAT	TGGCTTAGAAGACCCTTGGTT

Table 6. Antibodies

Antibody	Source	Dilution
Htt	Millipore cat. MAB2166	1:5,000, TBSt
Gapdh	Millipore cat. MAB374	1:2,000, 1% milk

Figures

Figure1. Huntington's Disease

A. The genetic defect causing the disease is an expansion of CAG triplet in the Huntingtin (Htt) gene. Up to 35 CAG repeats are included in the wild-type (wt) form of huntingtin (HTT) protein. Wt HTT has several benefic effects on neuron cell (top); more than 36 CAG repeats are associated with the mutated version of the protein, mHTT (bottom). Formation of mHTT caused neuronal degeneration and death. Image from *eurostemcell.org*.

B. Several cellular changes are associated with mHTT: in the cytoplasm it causes impairment of calcium signaling, mitochondrial damage and inhibition of protein clearance pathways. At nuclear level toxic fragments impair gene transcription or form intranuclear inclusions. Alterations in vesicular transport and recycling and excitoxicity are also reporterd. Image from Zuccato C, 2010.

Figure 1

A

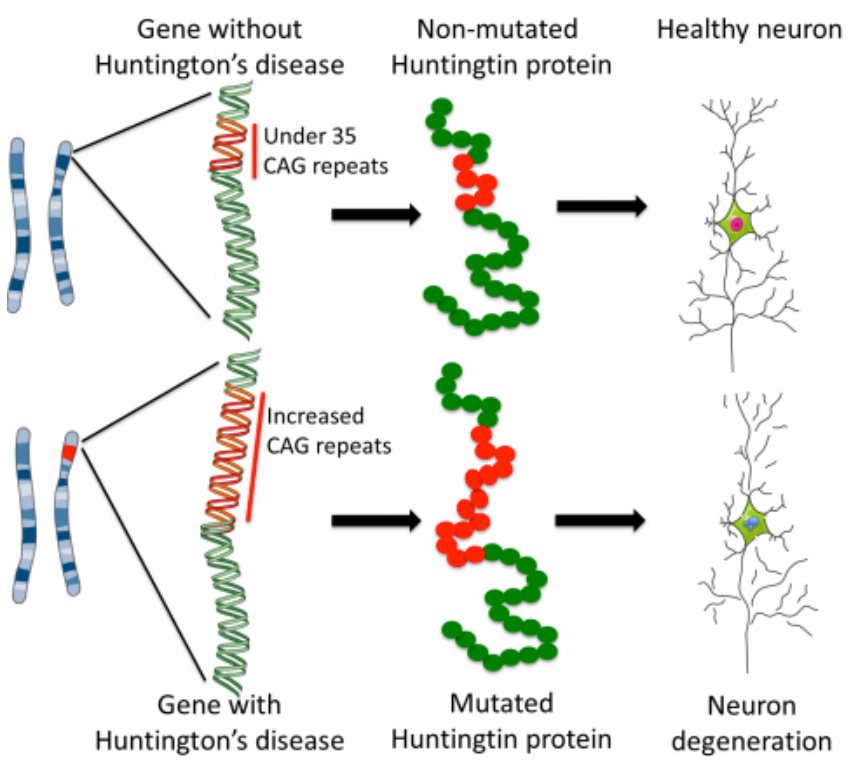
Gene without Huntington's disease
Non-mutated Huntingtin protein
Healthy neuron
Under 35 CAG repeats
Increased CAG repeats
Gene with Huntington's disease
Mutated Huntingtin protein
Neuron degeneration

B

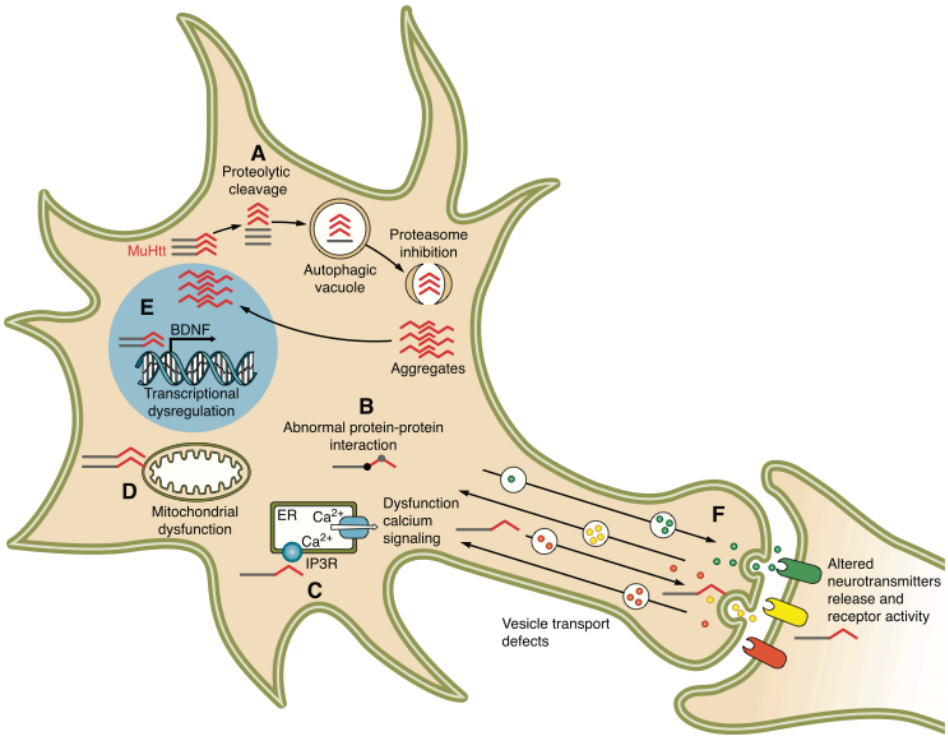
A
Proteolytic cleavage
MuHtt
Autophagic vacuole
Proteasome inhibition
E
BDNF
Transcriptional dysregulation
Aggregates
B
Abnormal protein-protein interaction
D
Mitochondrial dysfunction
ER
Ca2+
IP3R
C
Dysfunction calcium signaling
F
Vesicle transport defects
Altered neurotransmitters release and receptor activity

Figure 2. Genome-wide screen with mouse ES cells

A. Schematic representation of a general strategy for genome-wide screening in ES cells (adapted from Leeb M, 2014). The first step of the screening strategy is the generation of a mutant library upon genome-wide mutagenesis. After selection of mutants dysplaying the phenotype of interest, mutated locus were identified in each mutant clone. Final validation would prove that such phenotype is dependent on pB integration.

B. piggyBac transposon system includes pB vector and transposase enzyme which binds inverted terminal repeat sequences (ITRs) and mediates random integration of pB vector into genomic TTAA sites. pB vector can be excise without leaving footprint. Image from *bioscience.co.uk*.

Figure 2

A

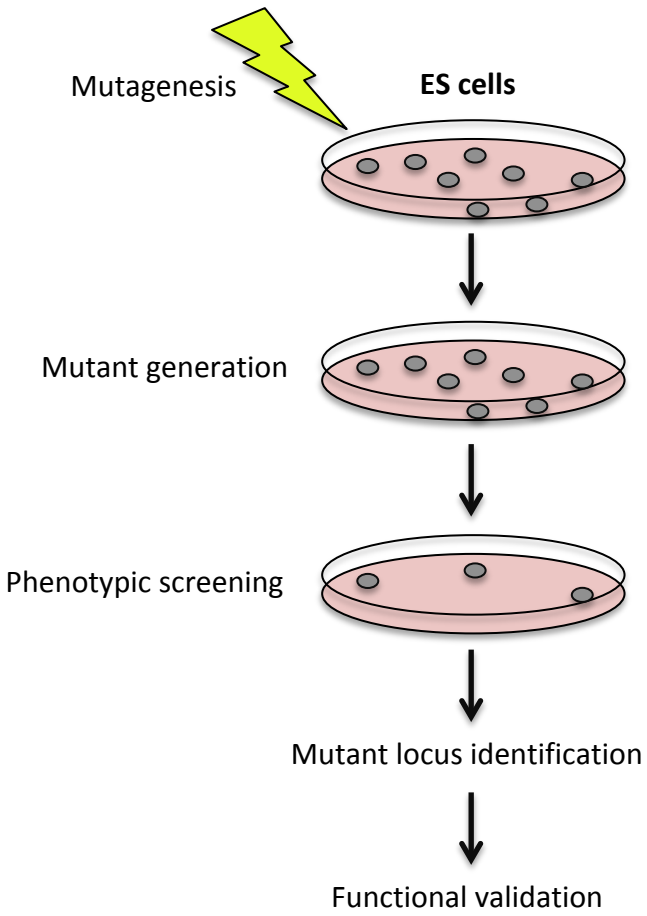
Mutagenesis
ES cells
Mutant generation
Phenotypic screening
Mutant locus identification
Functional validation

B

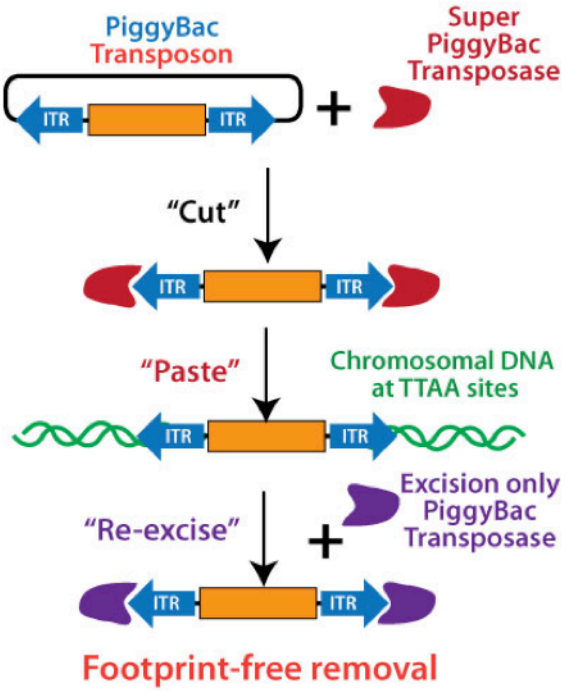
PiggyBac Transposon
Super PiggyBac Transposase
ITR
ITR
+
"Cut"
ITR
ITR
"Paste"
Chromosomal DNA at TTAA sites
ITR
ITR
"Re-excise"
Excision only PiggyBac Transposase
+
ITR
ITR
Footprint-free removal

Figure3. Generation and characterization of SRF-GFP reporter ES cell.

A. SRF-GFP reporter is used for monitoring SFR activity. MAL is predominantly localized in the cytoplasm, where it is sequestered by actin monomers. Either serum or mechanical stress (and Rho activation) induces MAL translocation into the nucleus, where it can associate with SRF in order to activate transcription of target genes.

Electroporation of SRF reporter on E14 cells generated SRF-GFP ES cells.

B. SRF reporter activation test. From left to right, GFP profiles of SRF-GFP ES cells cultured in N2B27 medium and in presence of 15% FBS or 2uM Cytochalasin D (CD). SRF reporter responds to both serum and cytoskeletal inputs, as showed by GFP signal enhancement of 24.1 and 86%, respectively. SRF-GFP ES cells cultured in N2B27 are used as control.

C. SRF reporter inactivation test. Two independent siRNAs targeting SRF (named siSRF1 and SRF2) and a control siRNA were transfected on SRF-GFP ES cells: CD treatment rapidly induced reporter activity in SRF-GFP ES cells transfected with control siRNA (top, right) while siSRF1 and siSRF2 successfully knock-down GFP signal also in the presence of CD (bottom). Un-transfected cells showed no GFP signal (top, left) and were used as negative control. All cell lines were cultured in N2B27 serum free media.

D. Upon siRNA-mediated knock-down of SRF, endogenous SRF target Tagln were found downregulated by qPCR, while it resulted upregulated in presence of CD. Data confirmed dependency of reporter activity on SRF levels.

Figure 3

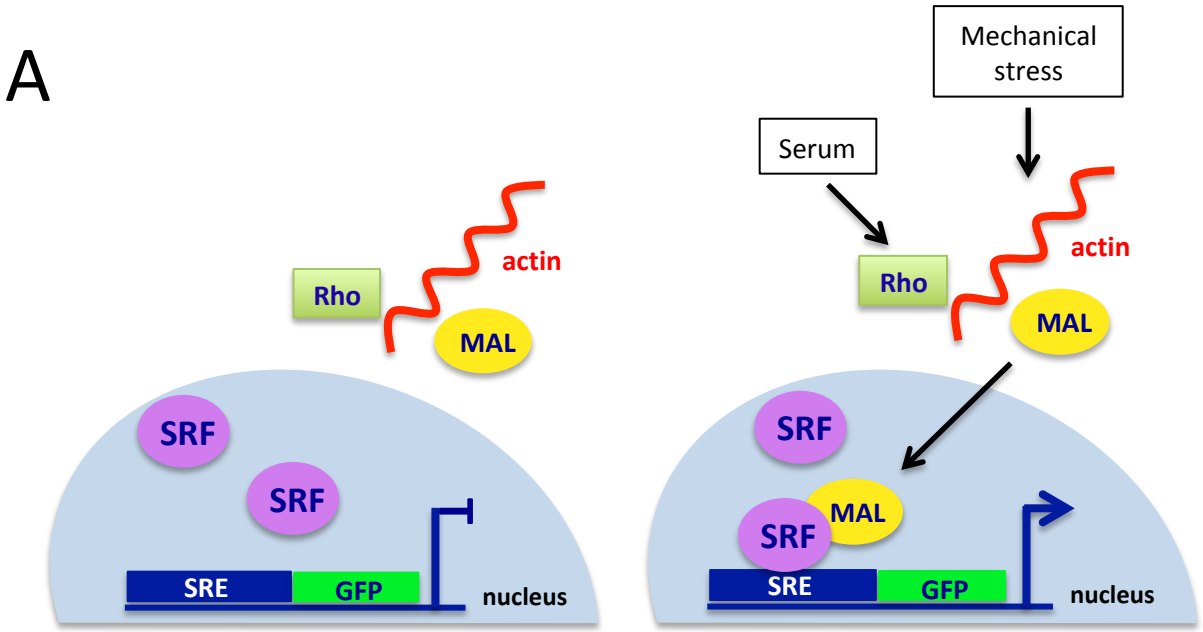
A
Mechanical stress
Serum
Rho
actin
MAL
SRF
SRF
SRE
GFP
nucleus
Rho
actin
MAL
SRF
SRF
MAL
SRE
GFP
nucleus

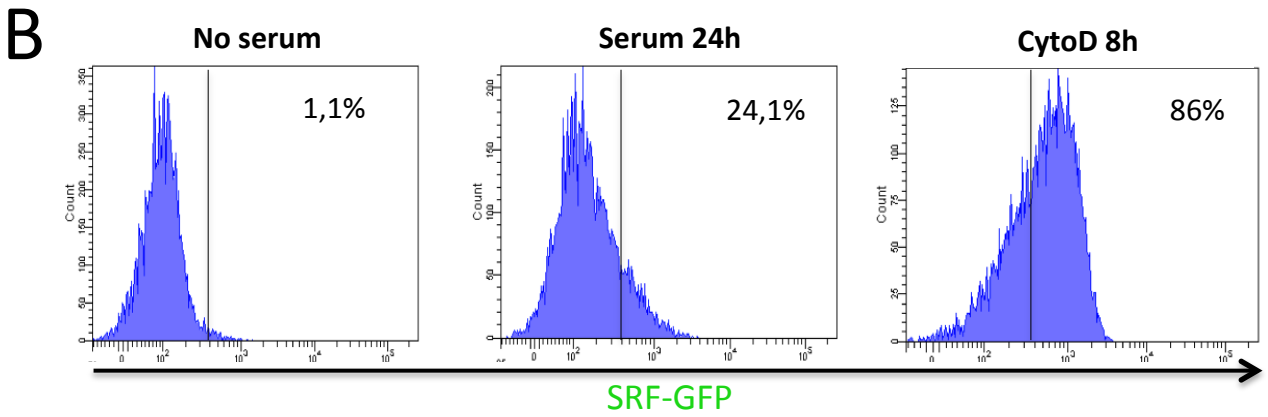
B
No serum
1,1%
Serum 24h
24,1%
CytoD 8h
86%
Count
SRF-GFP

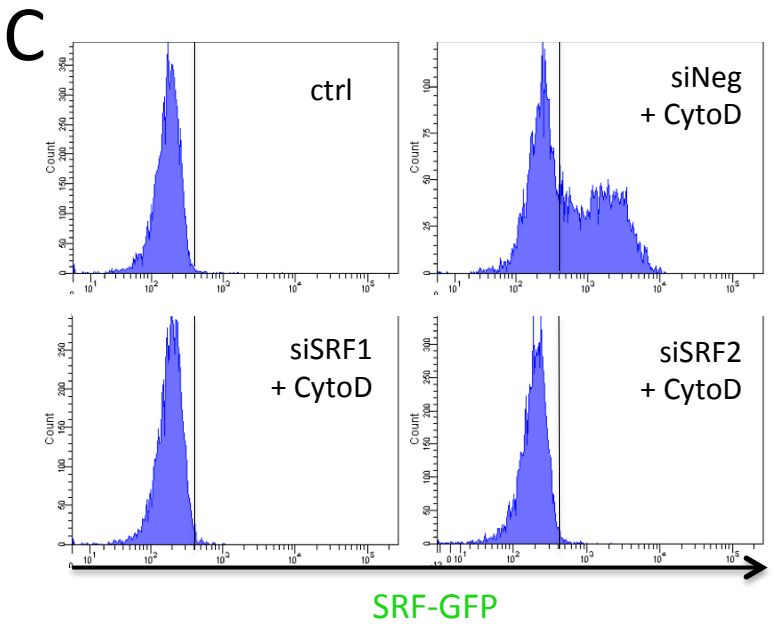
C
ctrl
siNeg
+ CytoD
siSRF1
+ CytoD
siSRF2
+ CytoD
Count
SRF-GFP

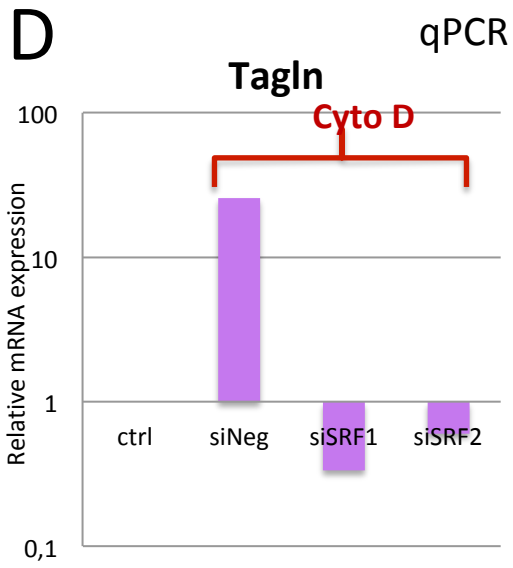
D
qPCR
Tagln
Cyto D
Relative mRNA expression
100
10
1
0,1
ctrl
siNeg
siSRF1
siSRF2

Figure 4. Genome-wide screen for novel regulators of SRF signaling

A. Diagram of endogenous gene activation by randomly integrated pGG134 vector containing the MSCV enhancer (Guo et al., 2010). This construct can activate nearby genes in either orientations (see text for details). DsRed and Hygromycin cassette is used to identify cells with successful vector integration.

B. Schematic representation of genome-wide screen strategy for novel regulators of SRF signaling.

C. Flow cytometry analysis showing that upon mutagenesis in serum-free culture condition, most (>85%) of cells were DsRed positive (top left quadrant) and among DsRed positive population, a small fraction (~1%) of cells was also positive for the SRF-GFP reporter (red dots in P3 region), indicating that successful activation of the reporter due to pB integrations.

Figure 4

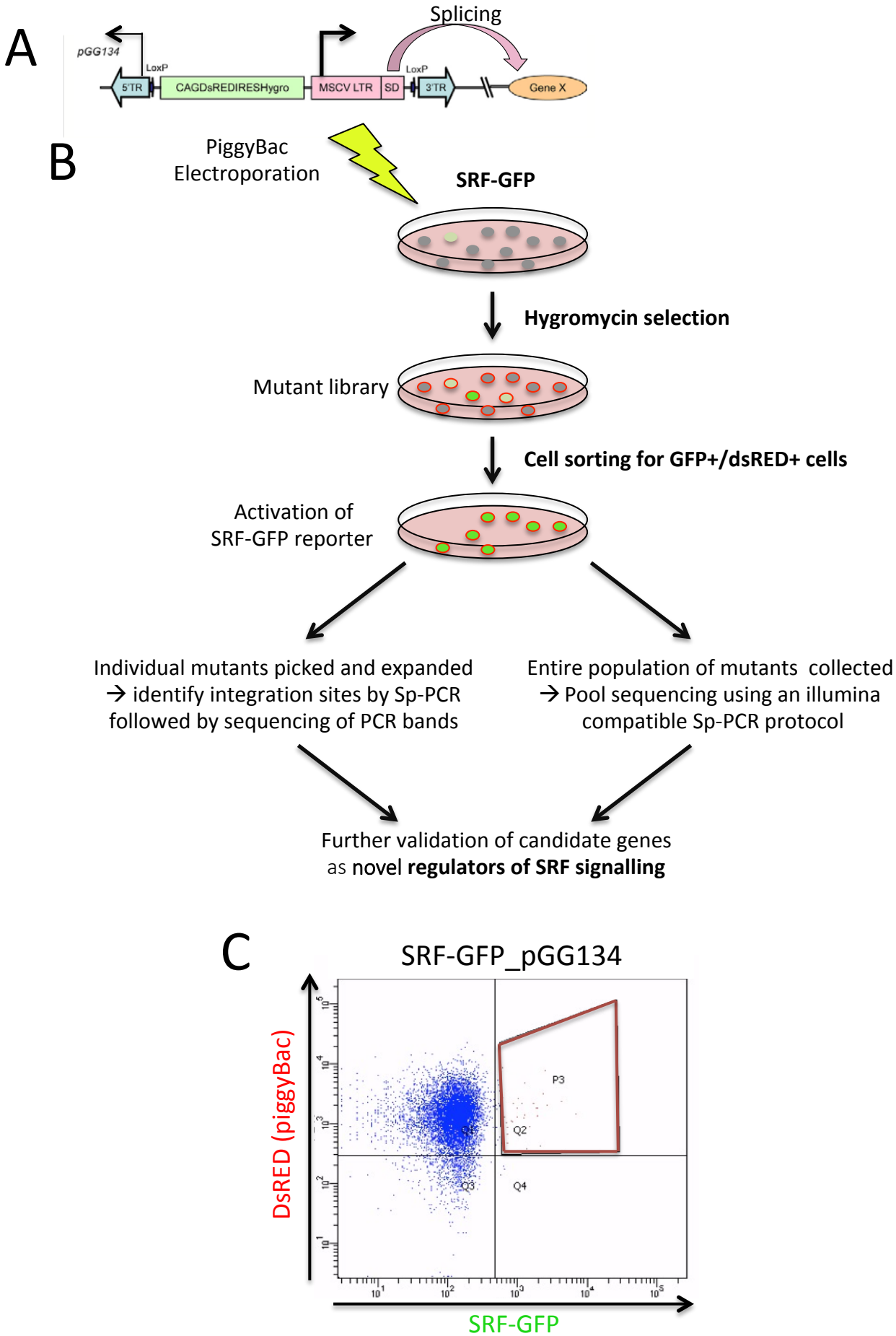
A
pGG134
LoxP
5'TR
CAGDsREDIRESHygro
MSCV LTR
SD
LoxP
3'TR
Gene X
Splicing
B
PiggyBac
Electroporation
SRF-GFP
Hygromycin selection
Mutant library
Cell sorting for GFP+/dsRED+ cells
Activation of
SRF-GFP reporter
Individual mutants picked and expanded
→ identify integration sites by Sp-PCR
followed by sequencing of PCR bands
Entire population of mutants collected
→ Pool sequencing using an illumina
compatible Sp-PCR protocol
Further validation of candidate genes
as novel regulators of SRF signalling
C
SRF-GFP_pGG134
DsRED (piggyBac)
SRF-GFP
P3
Q2
Q3
Q4

Figure 5. Identification of overactivated genes in resistant clones

A. Schematic overview of Splinkerette-PCR (Sp-PCR) products.

B-D. The gel electrophoresis in (B) shows Sp-PCR products from mutant clones B10-B13. Single band (red square) corresponding amplification of 5' end of the pB vector in B11, was excised from gel, purified and sequenced. The sequence obtained (C) includes a portion of genomic DNA (red) followed by BstYI restriction site (GATC sequence, black) and the adapter sequence (blue). Genomic sequence was then aligned to the mouse genome, allowing identification of Xbp1 gene upstream pB integration in clone B11.

E. List of targets identified by repeating Sp-PCR and analysis of PCR bands for all clones collected from SRF screening.

Figure 5

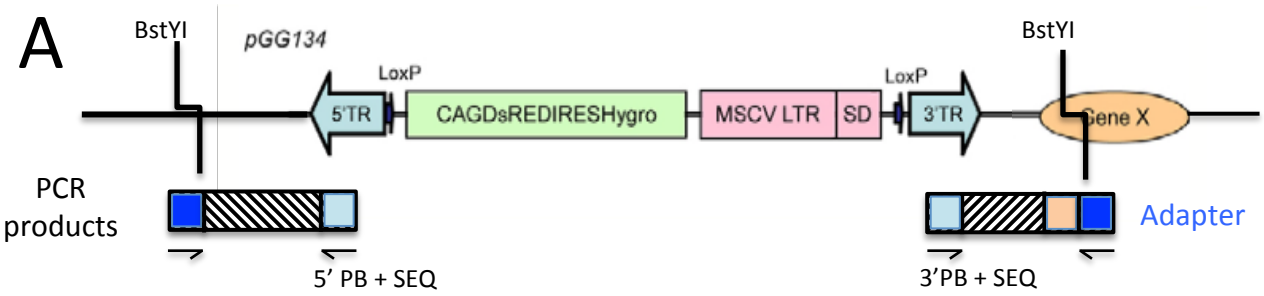

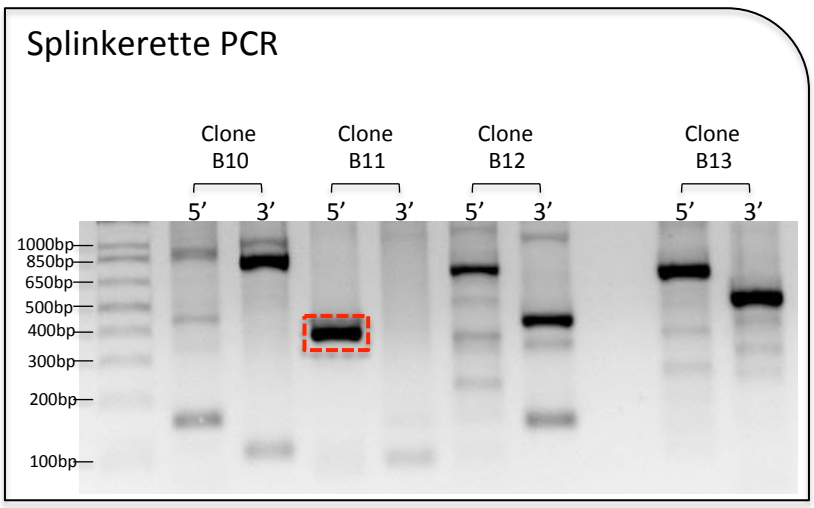

C

5' PB Sanger sequencing

TACATGGCCTAGGCTCAGTCTATAGCA
CTGAACAGCAAGCAAACCCAGCCTCCT
ATTCCTCCCTTCCCTTGGGCTTTACATAA
AACAAAACAAAACAAAACAAAACAAAA
CAAACAACAACAAAACCTGTGTATGAG
TGTTTTGCCGGCATGTATGTGTGCCCAT
CACATTTGTGTGTGGTGCCCATGGAGG
CTGAAAGACAGGCACTG**GATC**CCACTA
GTGTCGACACCAGTCC

Genomic DNA
BstYI site adapter

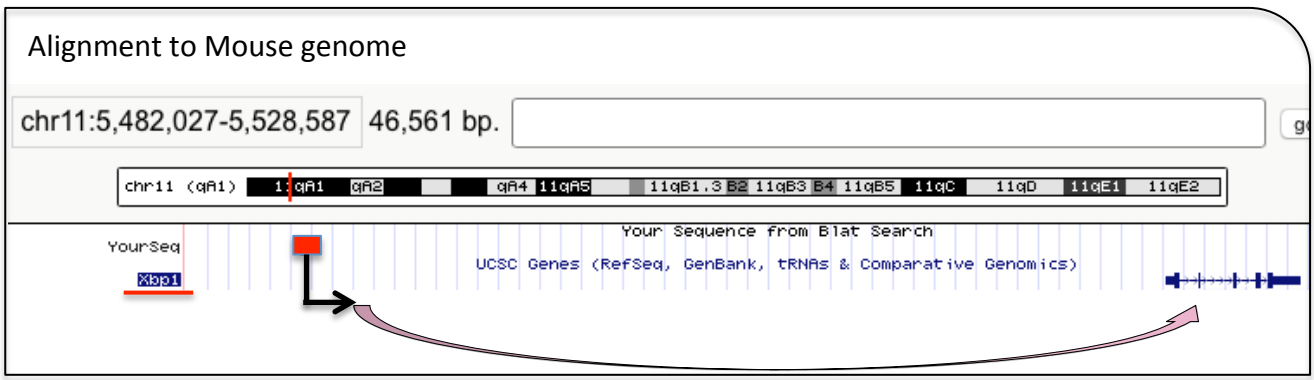

E

Mutant clone	Gene id by Sp-PCR
B3	Adgrl2
C44	Arf1
C23	Arhgap42
C17	Bbs9
A1	Dedd2
B5 C4 C11 C15 C18 C19 C28 C30 C32 C43 C47	Egfem1
C39	Ehbp1
B7 C6	Epb4.1l3
C9 C10	Fam20c
A6	Fcer2a
B13	Gm525

Mutant clone	Gene id by Sp-PCR
B10 C39	Kctd5
A8	Mbnl1
A13	Pcdh15
A15	Slc24a2
C21	Slc2a1
B2	Stambp
C16 C29	Tmem214
B11	Xbp1
C14	Ypel1
A4	asRNA
A11	Fat3

Figure 6. Validation of mutants of interest

A. Clones generated by genome-wide mutagenesis and enrichment by selection were analysed by flow cytometry for the percentage of GFP and DsRed positive cells. From left to right: parental SRF-GFP ES cells SRF-GFP_EV (empty vector) and selected mutants cultured in N2B27 serum free medium (percentage of GFP and DsRed double positive cells for each clone is indicated). All clones analysed displayed high levels of DsRed and GFP signals, proving that pB vector stable integrated and activated SRF reporter.

B. Also endogenous SRF target genes resulted upregulated in the absence of serum, as shown by qPCR for Egr1. Data confirmed that SRF reporter activation was maintained for prolonged culture.

Figure 6

A

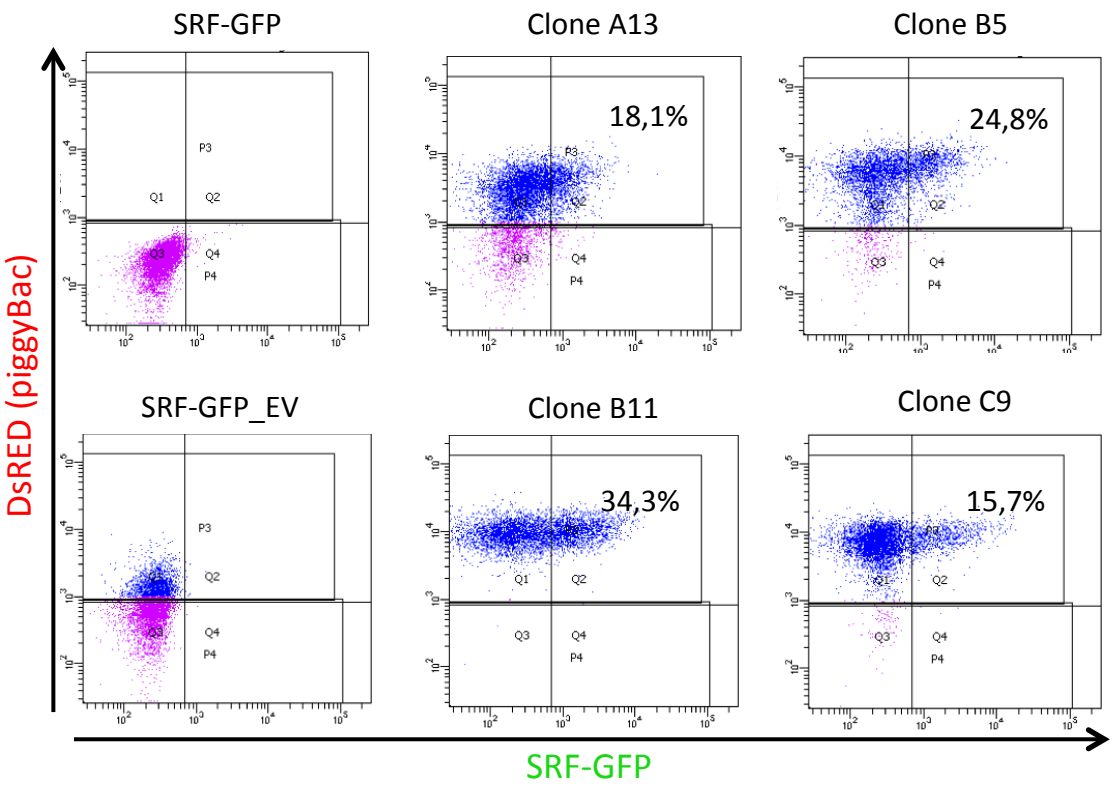
SRF-GFP
Clone A13
Clone B5
18,1%
24,8%
SRF-GFP_EV
Clone B11
Clone C9
34,3%
15,7%
DsRED (piggyBac)
SRF-GFP

B

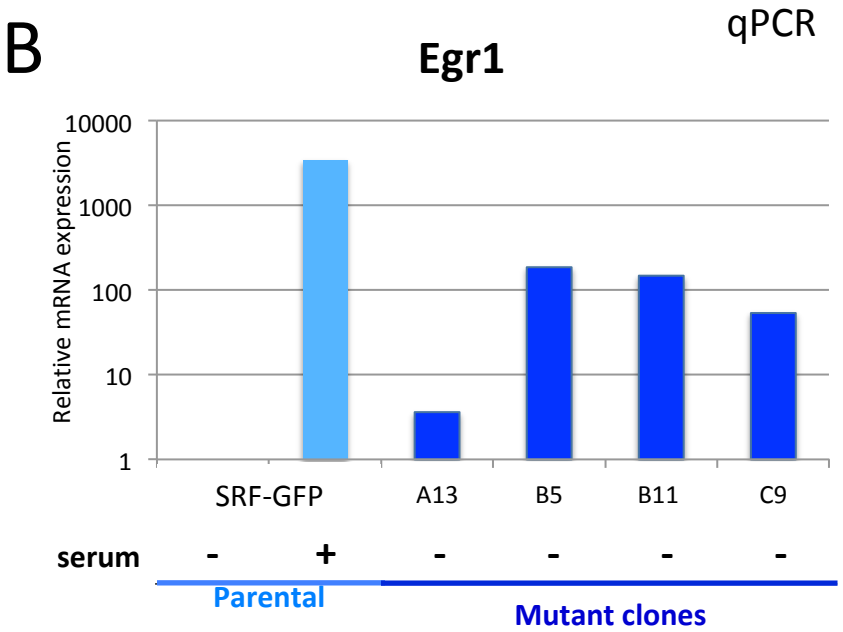
qPCR
Egr1
Relative mRNA expression
10000
1000
100
10
1
SRF-GFP
A13
B5
B11
C9
serum
- + - - - -
Parental
Mutant clones

Figure 7. Characterization of HD lines generated

A. qPCR analysis for Htt gene in Q15 Htt and Q128 Htt ES cells, compared to parental ES line, showed similar higher expression levels of Htt mRNA for both HD lines.

B. Western Blot of mutant HTT confirmed the correct production of a 80kDa and a 65kDa form of Htt protein in Q128 and Q15 cells Htt, compared to parental ES line. GAPDH was used as loading control. Of note, 348kDa wild type Htt protein could not be detected in experimental condition used.

C. Proliferation assay of Q128 Htt and Q15 Htt ES cells showed pronounced impairment in cell proliferation due to mutant Htt expression. Mean and s.e.m. of three independent experiments are shown.

D. ES cells expressing Q128 Htt showed impairment in proliferation ability. Treatments with exogenous stressors could exacerbate mutant Htt toxicity and induce cell death. To find such compounds would be the ideal condition to perform gain-of-function screening for identifying rare mutants surviving mutant Htt alterations.

Figure 7

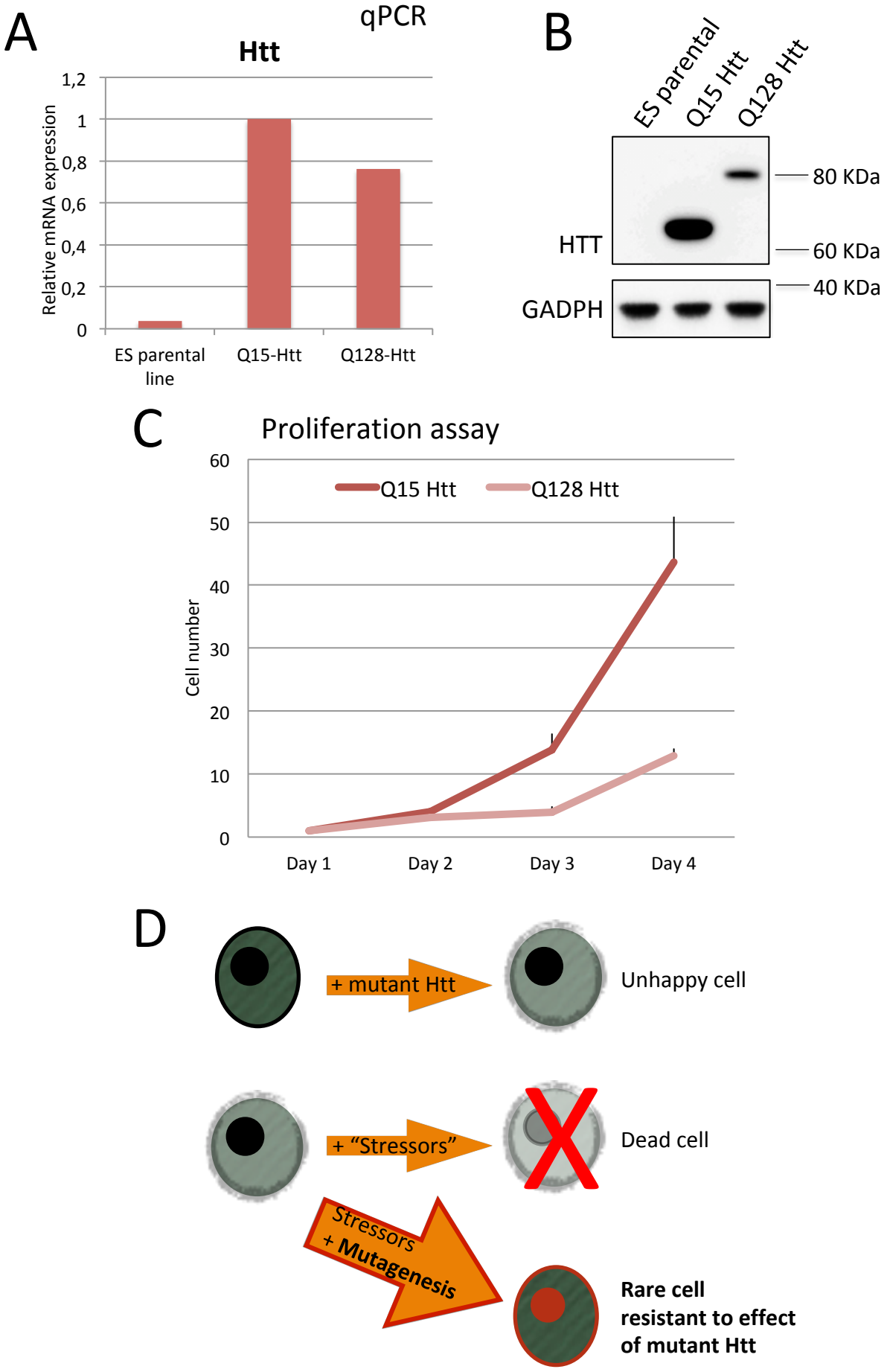
A
qPCR
Htt
Relative mRNA expression
1,2
1
0,8
0,6
0,4
0,2
0
ES parental line
Q15-Htt
Q128-Htt
B
ES parental
Q15 Htt
Q128 Htt
80 KDa
60 KDa
40 KDa
HTT
GADPH
C
Proliferation assay
Q15 Htt
Q128 Htt
Cell number
60
50
40
30
20
10
0
Day 1
Day 2
Day 3
Day 4
D
+ mutant Htt
Unhappy cell
+ "Stressors"
Dead cell
Stressors
+ Mutagenesis
Rare cell
resistant to effect
of mutant Htt

Figure 8. Effect of selected cellular stressors on HD lines

A. Panel of inhibitors tested and titrated in parental ES cells to find doses that were not lethal after 48 hours of treatment (right column).

B. Number of surviving cells quantified by Crystal Violet staining upon 48 hours of treatment with the selected compounds (from top to bottom): Rotenone, 3-MA, Bafilomycin A1 and Chloroquine were extremely toxic for both Q15 and Q128 Htt ES cells; MG132 and Tamoxifen (bottom panels) induced cell death in Q128 Htt cells.

Figure 8

A

Compound	Biological effect	Sublethal dose in ESCs
3-methyladenine	Autophagy inhibition	5 mM
Bafilomycin A1	Autophagy inhibition	3 nM
Chloroquine	Autophagy inhibition	12,5 uM
Hydrogen peroxide	Oxidative stress	25 uM
MG132	Proteasome inhibition	25 nM
Rotenone	Complex I inhibitor	200 nM
Tamoxifen	Estrogen response modifier	11 uM

B

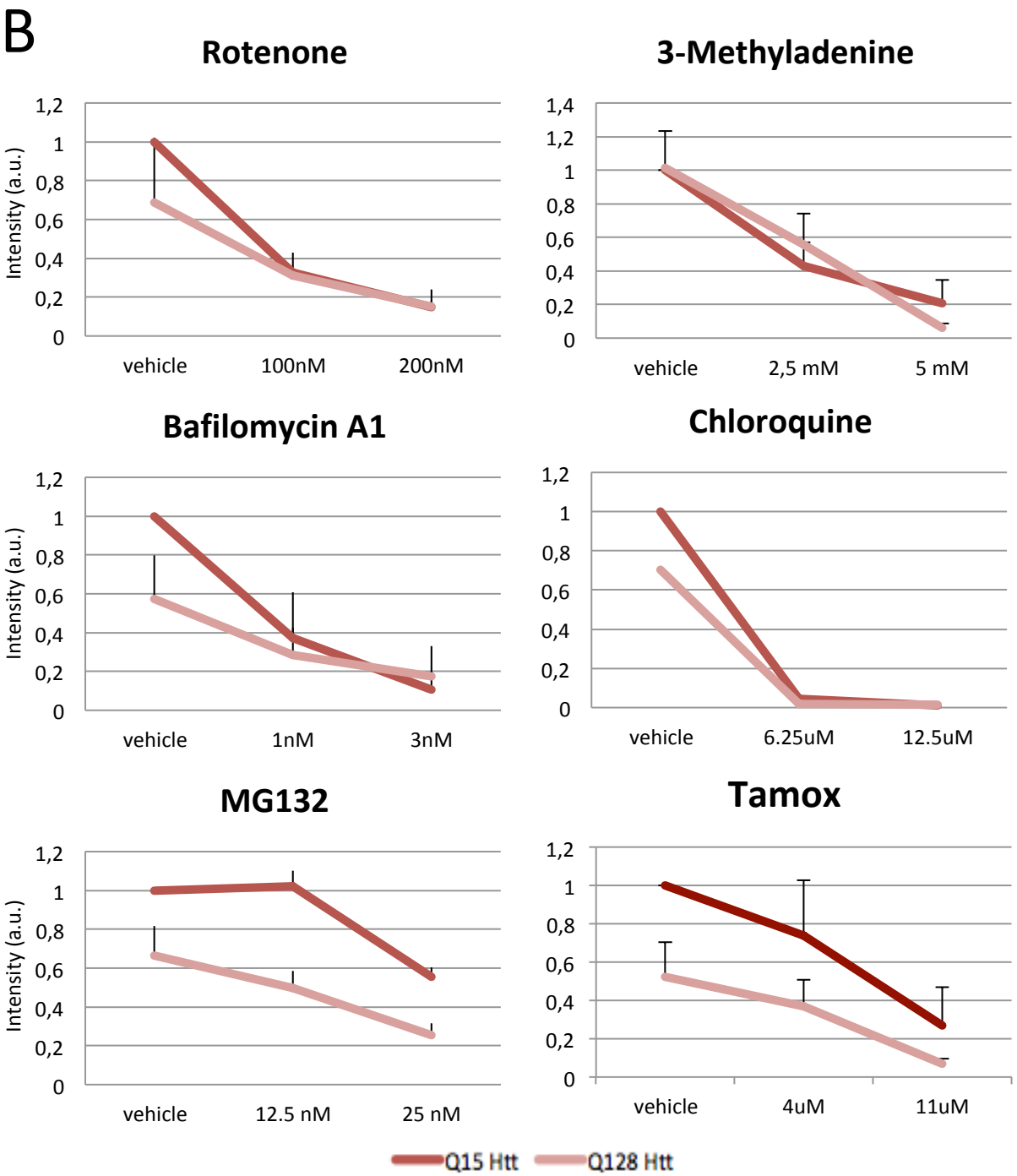

Figure 9. Screening strategy used to identify new proteins involved in Htt-dependent toxicity

Figure 9

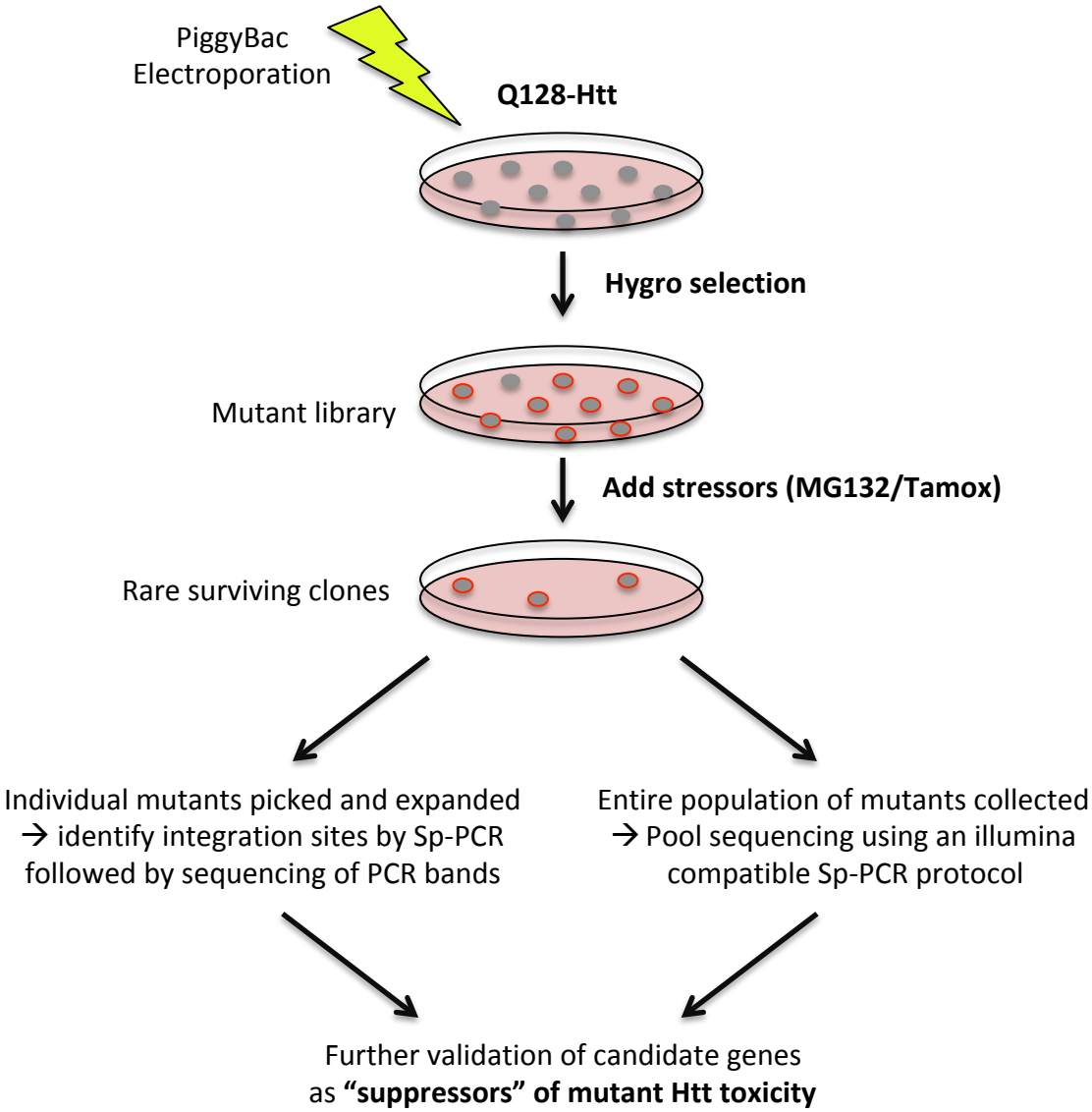
PiggyBac
Electroporation
Q128-Htt
Hygro selection
Mutant library
Add stressors (MG132/Tamox)
Rare surviving clones
Individual mutants picked and expanded
→ identify integration sites by Sp-PCR
followed by sequencing of PCR bands
Entire population of mutants collected
→ Pool sequencing using an illumina
compatible Sp-PCR protocol
Further validation of candidate genes
as "suppressors" of mutant Htt toxicity

Figure 10. Genome-wide screen for new genes conferring resistance to mutant Htt

A. Representative Crystal Violet staining of parental ES cells electroporated with an empty pB (parental ES_EV on the left), Q128 Htt line electroporated with EV (Q128_EV in the middle) and Q128 Htt cells electroporated with pGG134 vector (Q128_pGG134 on the right) treated with MG132 for 5 days. Rare Q128_pGG134 cells survived to MG132 selection.

B and C. Number of surviving Q128_pGG134 colonies resulted significantly increased compared to Q128_EV from several rounds of mutagenesis and selection in presence of MG132 (B) or Tamoxifen (C). Data are presented as mean ± standard deviation from three independent experiments, unpaired *t*-test: $^{**}P < 0.01$.

D. Summary of number of entire populations of mutants and single clones collected from different mutagenesis/selection cycles with MG132 or Tamoxifen.

Figure 10

A

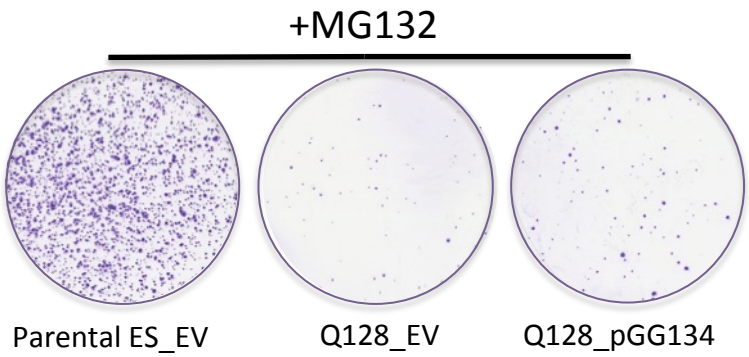

B

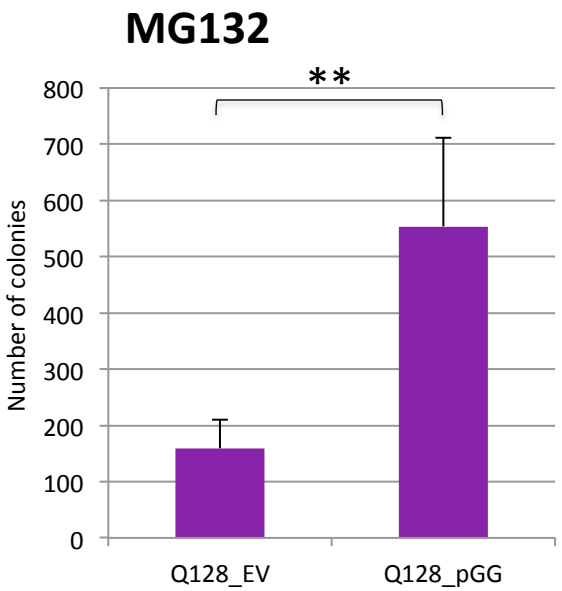

C

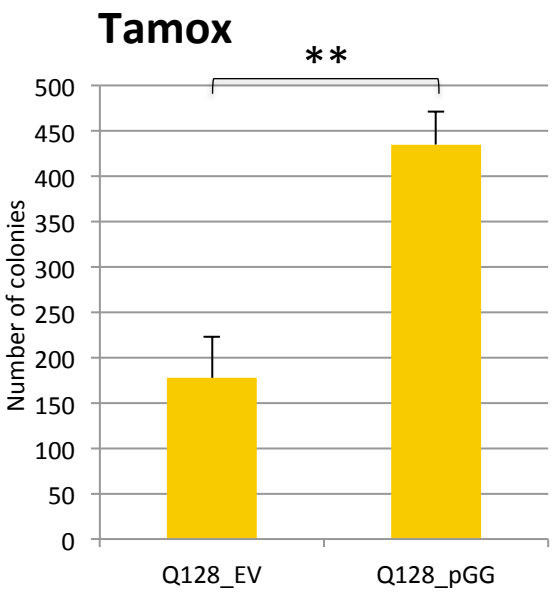

D

Number of	Selected in		Total
	MG132	Tamoxifen	
Populations	**10**	**7**	**17**
Mutant clones	**26**	**18**	**44**

Figure 11. Identification of overactivated genes in resistant clones

A. Schematic overview of Splinkerette-PCR products (see text for details of PCR procedure).

B-D. The gel electrophoresis in (B) shows Splinkerette-PCR products from mutant clones MG15, MG16 and MG17. Two major bands, highlighted in red and yellow, corresponded to amplification of 5' and 3' end of the pB vector integrated in clone MG15. Selected single PCR band (red square) was then excised from gel, purified and sequenced. The sequence obtained (C) includes a portion of genomic DNA (red) followed by BstYI restriction site (GATC sequence, black) and the adapter sequence (blue). Genomic sequence was then aligned to the mouse genome, allowing identification of the precise site of integration in each mutant cell line (D). Here, pB vector was found inserted upstream of the Kdm5b gene.

E. qPCR analysis for (top) Kdm5b, Qk, Fbxo34, (bottom) Mtf1, Synj2 and Arid1b genes identified by Sp-PCR, confirmed upregulated expression of such candidate targets in the corresponding clones, compared to both the parental and the Q128 Htt cell line.

Figure 11

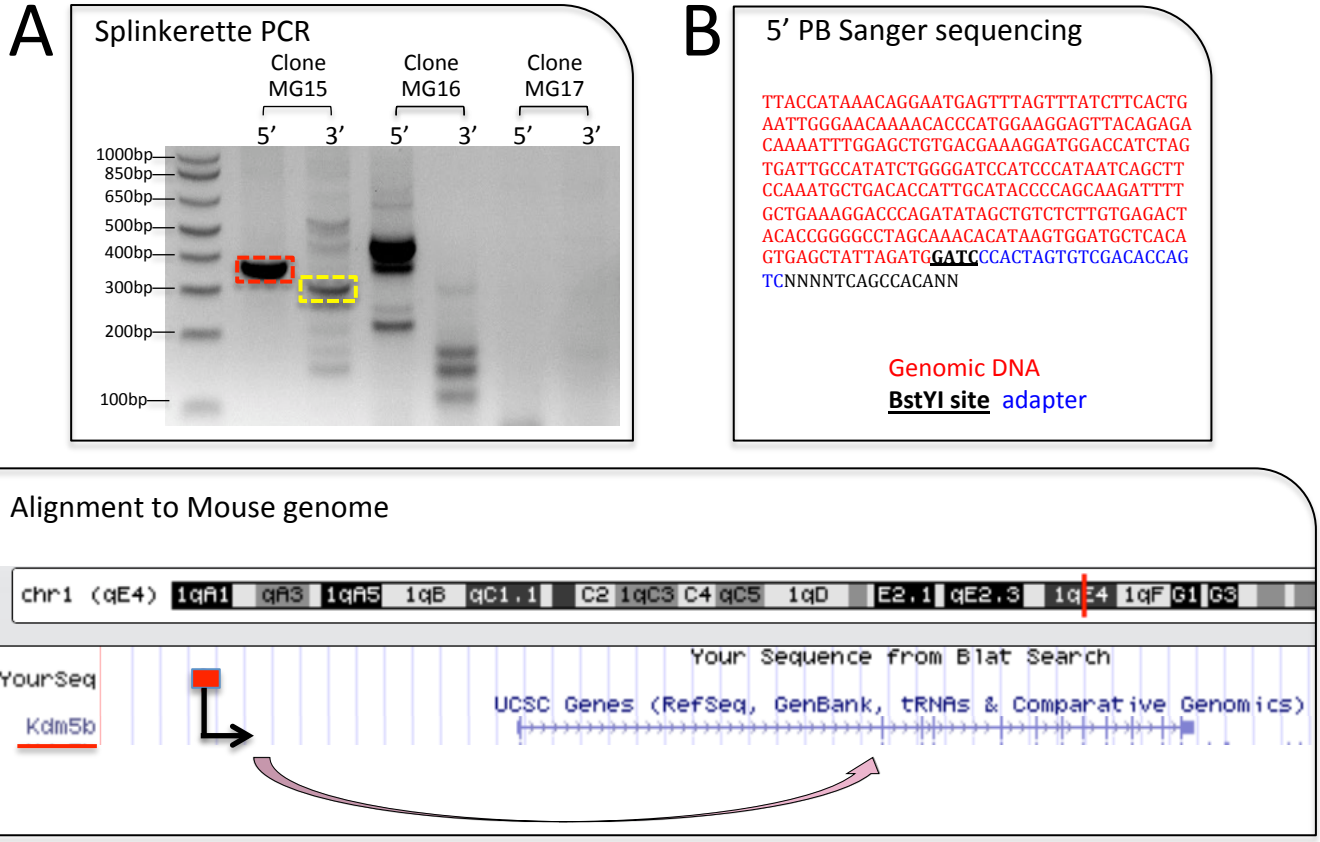
A
Splinkerette PCR
Clone MG15
Clone MG16
Clone MG17
5′ 3′ 5′ 3′ 5′ 3′
1000bp
850bp
650bp
500bp
400bp
300bp
200bp
100bp
B
5′ PB Sanger sequencing
TTACCATAAACAGGAATGAGTTTAGTTTATCTTCACTG
AATTGGGAACAAAACACCCATGGAAGGAGTTACAGAGA
CAAAATTTGGAGCTGTGACGAAAGGATGGACCATCTAG
TGATTGCCATATCTGGGGATCCATCCCATAATCAGCTT
CCAAATGCTGACACCATTGCATACCCCAGCAAGATTTT
GCTGAAAGGACCCAGATATAGCTGTCTCTTGTGAGACT
ACACCGGGGCCTAGCAAACACATAAGTGGATGCTCACA
GTGAGCTATTAGATGGATCCCACTAGTGTCGACACCAG
TCNNNNTCAGCCACANN
Genomic DNA
BstYI site adapter
C
Alignment to Mouse genome
chr1 (qE4)
YourSeq
Kdm5b
Your Sequence from Blat Search
UCSC Genes (RefSeq, GenBank, tRNAs & Comparative Genomics)
D
qPCR
Kdm5b
Qk
Fbxo34
Relative mRNA expression
ES parental
Q128_EV
clone MG15
clone MG3
clone MG21
Mtf1
Synj2
Arid1b
clone MG18
clone MG9
clone T4

Figure 12. Characterization of selected mutant clones

A. Representative Crystal Violet staining of Q128 Htt cells and 4 clones selected from Q128_pGG134 mutant population. All clones resulted resistant to lethal concentrations of exogenous stressors (top: MG132; bottom: Tamoxifen treatment) while Q128 Htt cells massively died. Parental ES cells survived.

B and C. Crystal violet quantification showing number of surviving colonies in all 6 clones in analysis after 48hrs of treatments with MG132 (B) and Tamoxifen (C). All lines showed significant increase proliferation ability in stressor conditions compared to Q128 Htt cells and parental ES cells, too.

D. qPCR analysis showed similar high expression levels of Htt mRNA in all clones, as well as in Q128 Htt ES cells, confirming that HttQ128 mRNA was not silenced over the entire procedure.

E. Western Blot of mutant HTT confirmed also that protein was not degradated in any clones.

Figure 12

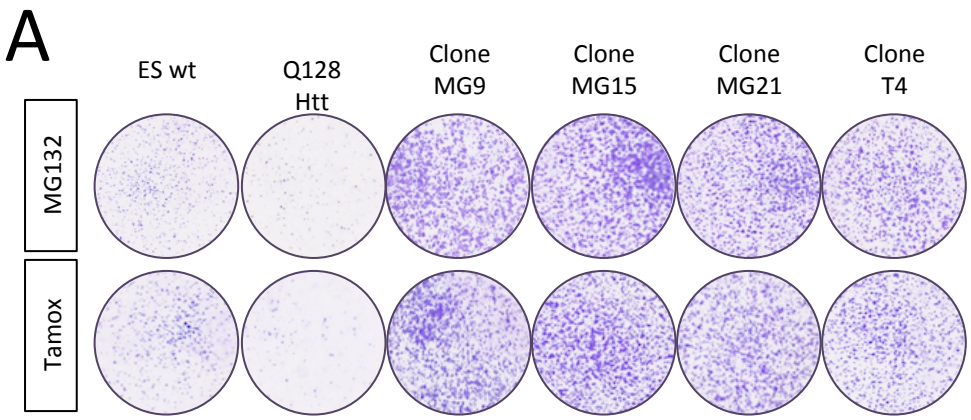
A
ES wt
Q128 Htt
Clone MG9
Clone MG15
Clone MG21
Clone T4
MG132
Tamox

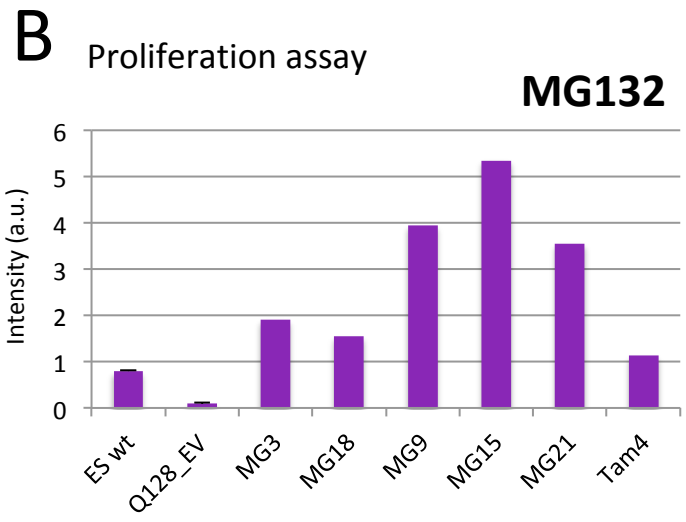
B
Proliferation assay
MG132
Intensity (a.u.)
0
1
2
3
4
5
6
ES wt
Q128_EV
MG3
MG18
MG9
MG15
MG21
Tam4

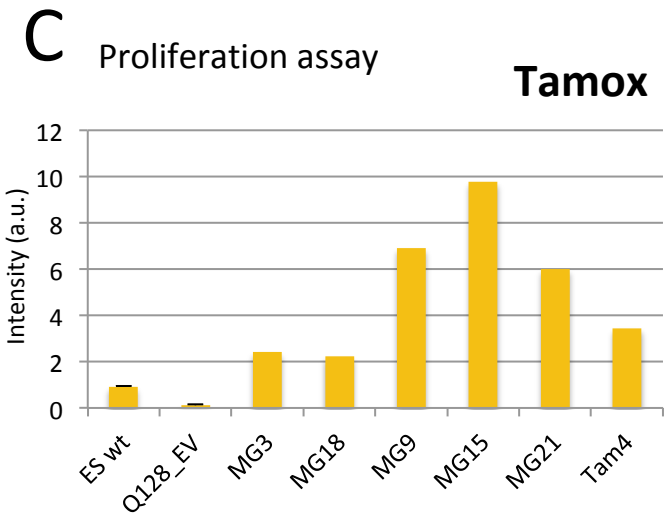
C
Proliferation assay
Tamox
Intensity (a.u.)
0
2
4
6
8
10
12
ES wt
Q128_EV
MG3
MG18
MG9
MG15
MG21
Tam4

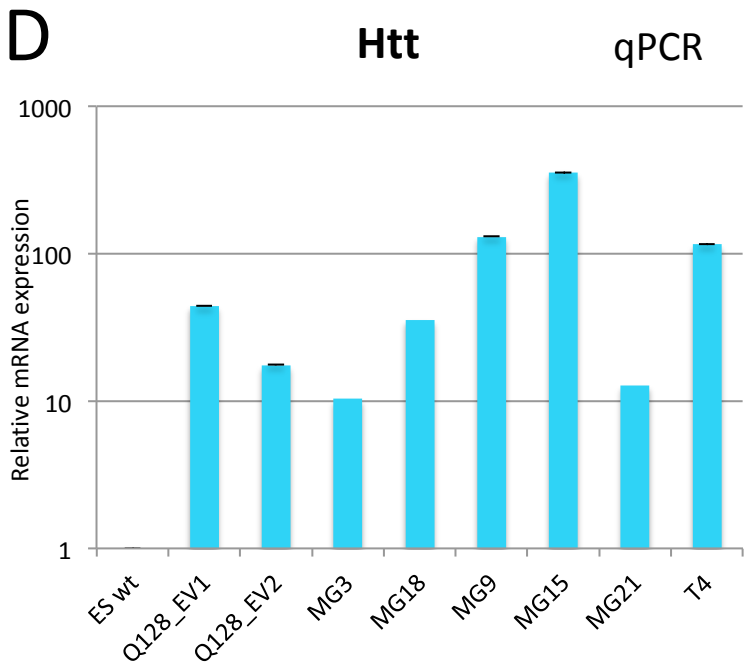
D
Htt
qPCR
Relative mRNA expression
1
10
100
1000
ES wt
Q128_EV1
Q128_EV2
MG3
MG18
MG9
MG15
MG21
T4

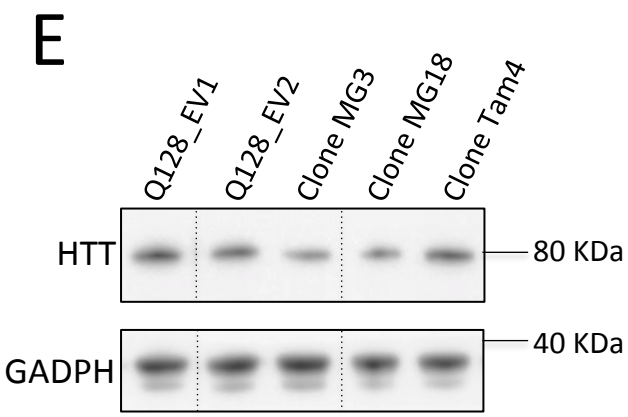
E
Q128_EV1
Q128_EV2
Clone MG3
Clone MG18
Clone Tam4
HTT
80 KDa
GADPH
40 KDa

Figure 13. Analyses of the pattern of integration of pB vectors in resistant clones

A. List of targets identified by repeating Sp-PCR and analysis of PCR bands for all MG or Tamoxifen clones collected.

B. Bioinformatic analysis of the list of mutated genes identified by Sp-PCR, grouped by molecular function. Results showed high representation of transcriptional regulators (30%).

C. Venn-diagram reporting comparative analysis of NGS data from two completely unrelated screenings (SRF versus HD).

D. Bioinformatic analysis of the list of mutated genes identified by NGS, grouped by molecular function. Results confirmed enrichment in transcriptional regulator category (20%).

Figure 13

A

Mutant clone	Gene id by Sp-PCR
MG2 MG3 MG4 MG5 MG6 T3 T12 T13	Qk
MG7	Arnt2
MG8	D930020B18Rik
MG9	Synj2
MG9	Chst5
MG10	Slc1a1
MG11	Cd163
MG12	Rab29
MG13 T17	Myo16
MG14	Npy5r
MG15	Kdm5b
MG16	LOC102636514
MG18	Mtf1
MG20	Epb41l3
MG21	Fbxo34
MG22	Trappc6b
MG23	Rev3l
MG24 T4 T7 T18	Fcer2a
T4	Arid1b
T6	Slc38a4
T7	Trak2
T8	Hdgf
T9	Pbld2
T10	Fat3
T11	Col19a1
T15	Plk3
T16	Wrn
T17	Scrt2
T18	Mctp2

B

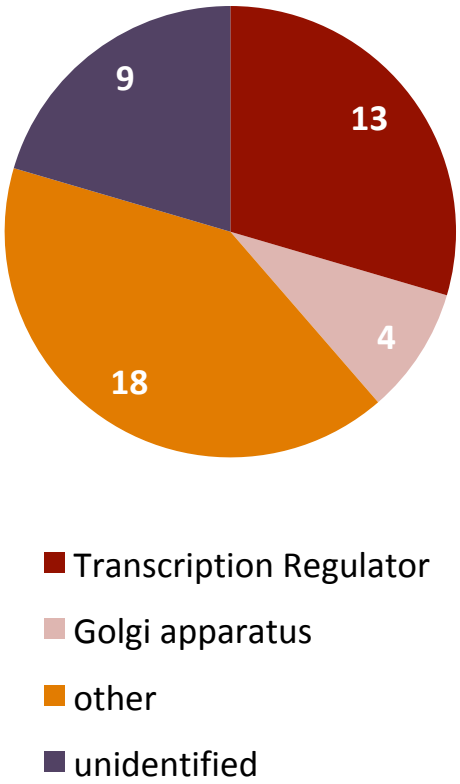

C

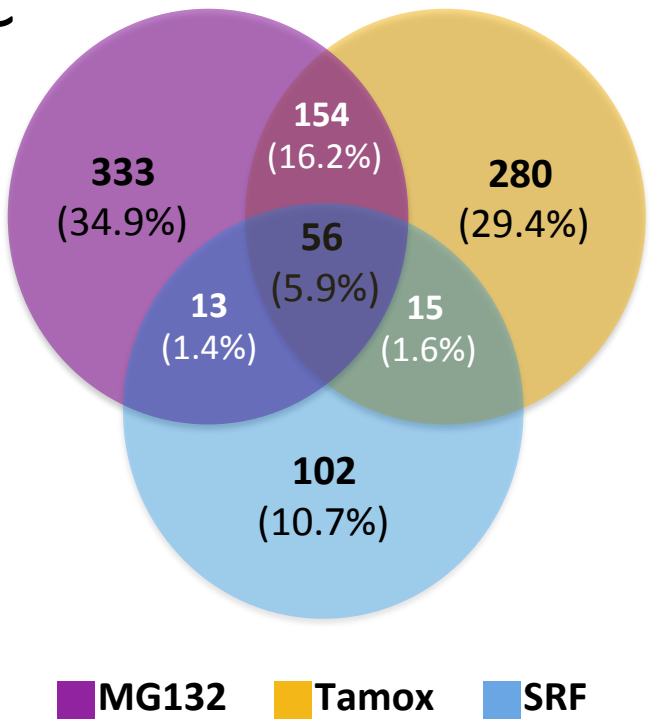

D

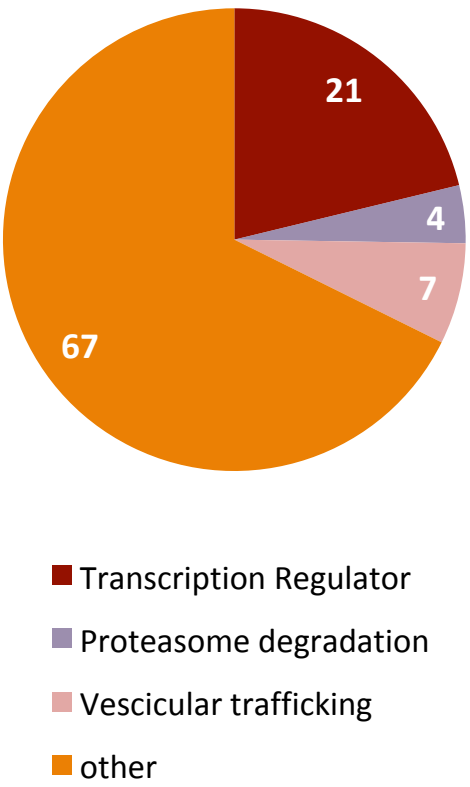

Figure 14. Validation of candidate genes as "suppressors" of mutant Htt toxicity (1)

A. Strategy used to test reversion of phenotype in selected clones. The hyphotesis was that clones would lose resistance upon pB excision.

B. Schematic view of excision of pB vector by CRE recombinase transfection in selected clones. CRE transfection would result in removal of the entire pB cassette including DsRed and Hygromycin resistance gene.

C. Flow cytometry analysis showing levels of DsRed expression in control ES cells (left), clones MG9 and MG15 (middle) and clones +CRE (right). Both clones showed decreased DsRed signal upon CRE transfection, while their un-transfected counterpart remained homogeneously DsRed positive.

D. Quantification of DsRed positive cells (%) detected by flow cytometry analysis for all mutant clones before and after pB excision. Wild-type and Q128 Htt ES cells were included as negative controls, while ES wt_EV as positive one. Transient CRE-transfection resulted in efficient pB-removal.

Figure 14

A

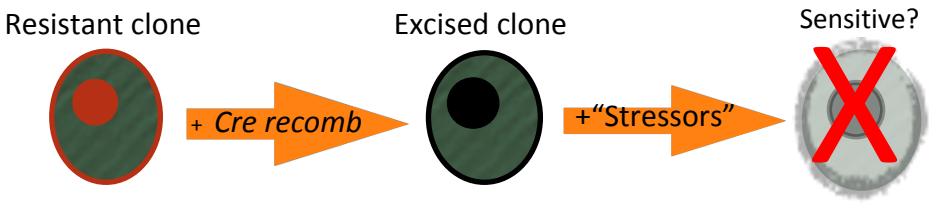

B

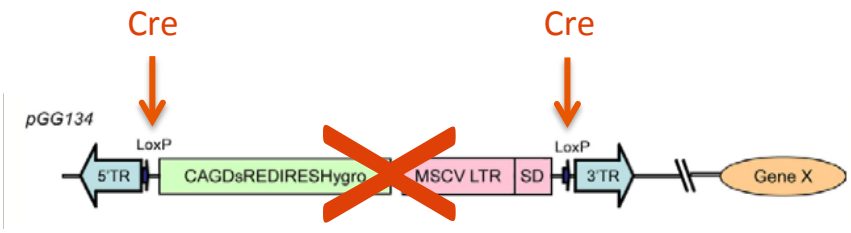

C

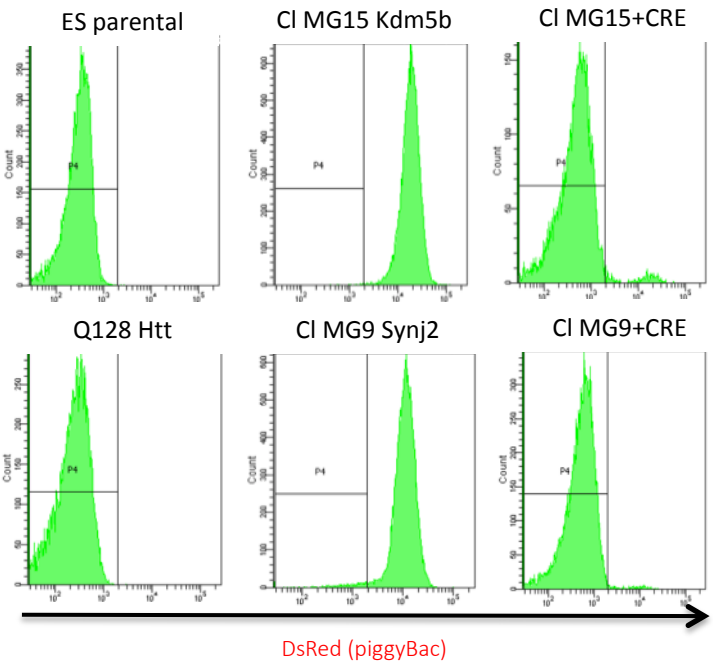

D

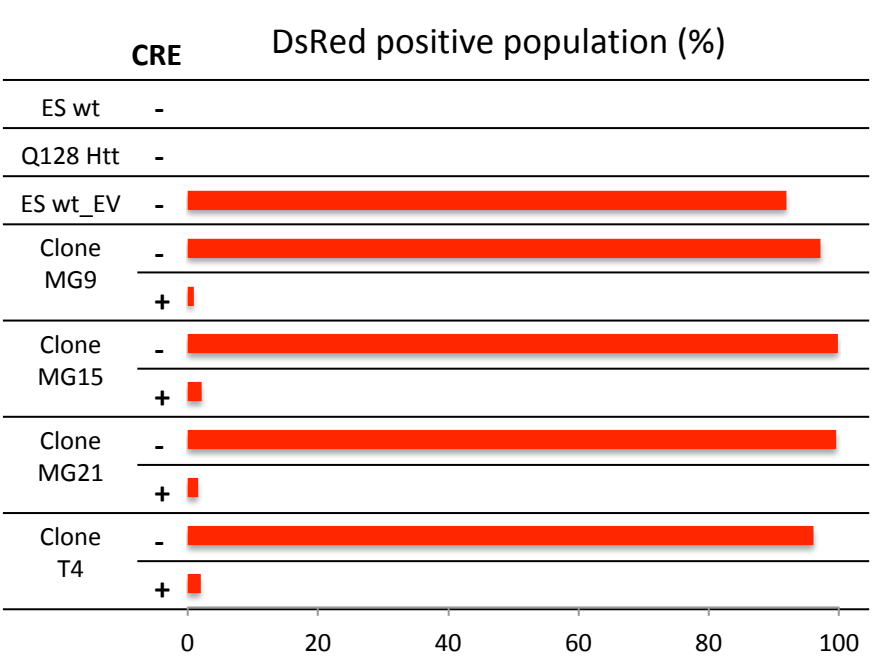

Figure 15. Validation of candidate genes as "suppressors" of mutant Htt toxicity (2)

A and B. Crystal violet quantification showing number of surviving colonies in clones±CRE after 48hrs of treatments with MG132 (E) and Tamoxifen (F). All the clones confirmed the phenotype (compare bars 3, 5, 7 and 9 vs 2). Clone MG15 and T4 showed significant decrease in cell survival after CRE-mediated excision (compare bars 6-5, and 10-9), confirming a pB-integration dependent phenotype. In contrast, MG9 or MG21 did not show the same (bars 4-3 and 8-7), suggesting the presence of some artefactual mechanism not related to mutagenesis. Data are presented as mean ± standard deviation from two independent experiments, unpaired *t*-test: **P* <0.05, ***P* <0.01.

C. Western Blot analyses for HTT protein proved that mutant Htt was still present in all the cell line, suggesting that increased survival observed in some clones had no effect on Htt expression.

Figure 15

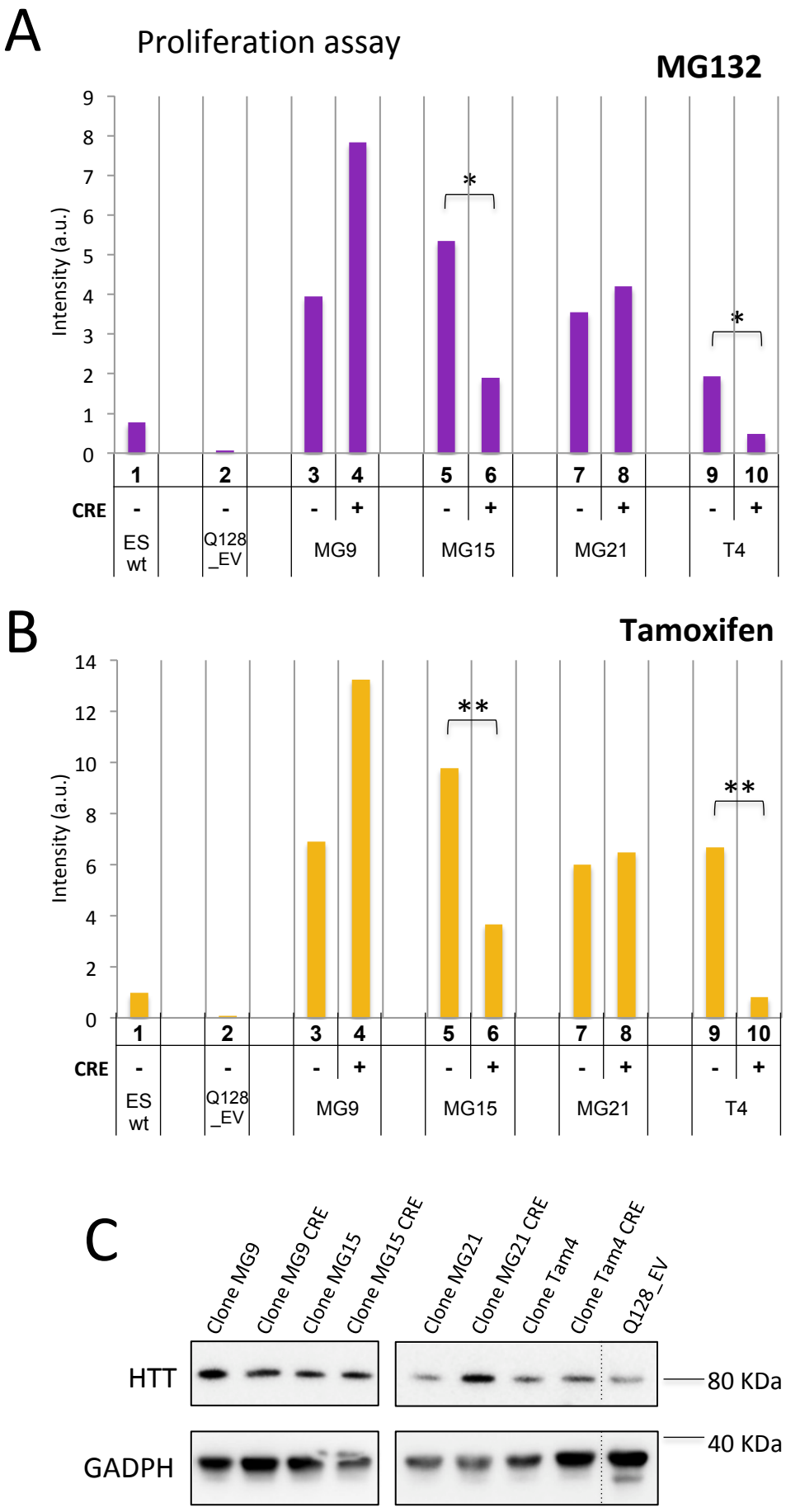
A
Proliferation assay
MG132
Intensity (a.u.)
0
1
2
3
4
5
6
7
8
9
*
*
1
2
3
4
5
6
7
8
9
10
CRE
-
-
-
+
-
+
-
+
-
+
ES wt
Q128 _EV
MG9
MG15
MG21
T4
B
Tamoxifen
Intensity (a.u.)
0
2
4
6
8
10
12
14
**
**
1
2
3
4
5
6
7
8
9
10
CRE
-
-
-
+
-
+
-
+
-
+
ES wt
Q128 _EV
MG9
MG15
MG21
T4
C
Clone MG9
Clone MG9 CRE
Clone MG15
Clone MG15 CRE
Clone MG21
Clone MG21 CRE
Clone Tam4
Clone Tam4 CRE
Q128_EV
HTT
GADPH
80 KDa
40 KDa

Figure 16. Independent validation of candidates as genes conferring resistance to Q128 cells (1)

A. Schematic representation of overexpression experiment performed by transfection on Q128 cells of a vector harboring cDNA of candidate genes under the control of a constitutive CAG promoter (Q128_candidate), or an empty vector that served as control (Q128_EV).

B and C. qPCR and Western Blot analyses for HttQ128 mRNA and protein proved that mutant Htt was properly produced in all the new cell lines generated.

D. qPCR analysis for Mtf1, Kdm5b and Fbxo34 confirmed increased levels of genes in corresponding cell lines in which they were overexpressed, compared to the parental ES cells.

E. Proliferation assay of Q128_Mtf1, Q128_Kdm5b and Q128_Fbxo cells compared to Q128 and Q15 Htt cells, showed increased proliferation upon Mtf1 a nd Kdm5b overexpression and no effect fro Fbxo34. Q128_EV cells displayed impaired proliferation relative to control Q15 cells

Figure 16

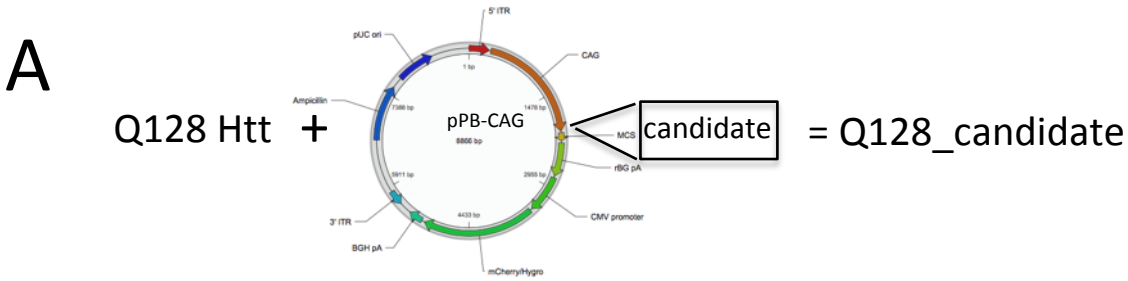
A
Q128 Htt
+
pPB-CAG
candidate
= Q128_candidate
5' ITR
pUC ori
CAG
Ampicillin
MCS
rBG pA
3' ITR
CMV promoter
BGH pA
mCherry/Hygro

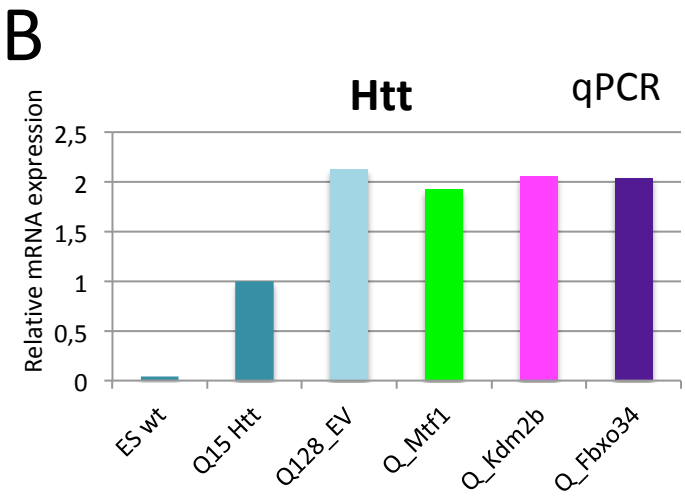
B
Htt
qPCR
Relative mRNA expression
2,5
2
1,5
1
0,5
0
ES wt
Q15 Htt
Q128_EV
Q_Mtf1
Q_Kdm2b
Q_Fbxo34

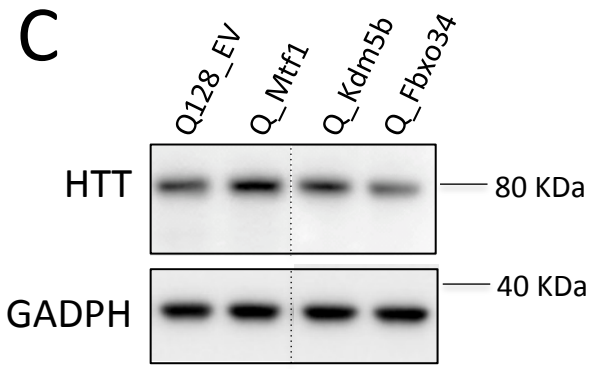
C
Q128_EV
Q_Mtf1
Q_Kdm5b
Q_Fbxo34
HTT
80 KDa
GADPH
40 KDa

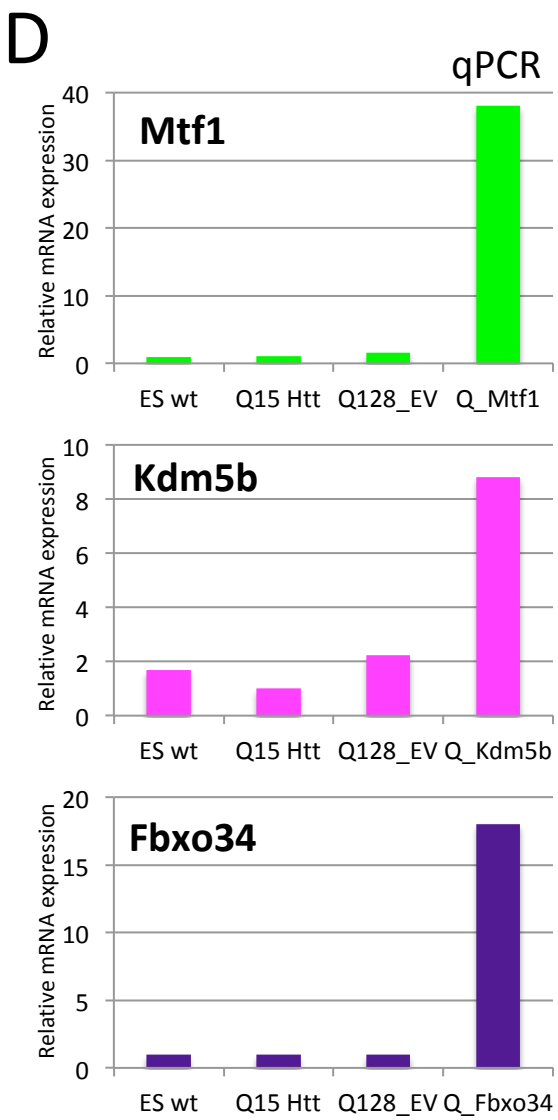
D
qPCR
Mtf1
Relative mRNA expression
40
30
20
10
0
ES wt
Q15 Htt
Q128_EV
Q_Mtf1
Kdm5b
Relative mRNA expression
10
8
6
4
2
0
ES wt
Q15 Htt
Q128_EV
Q_Kdm5b
Fbxo34
Relative mRNA expression
20
15
10
5
0
ES wt
Q15 Htt
Q128_EV
Q_Fbxo34

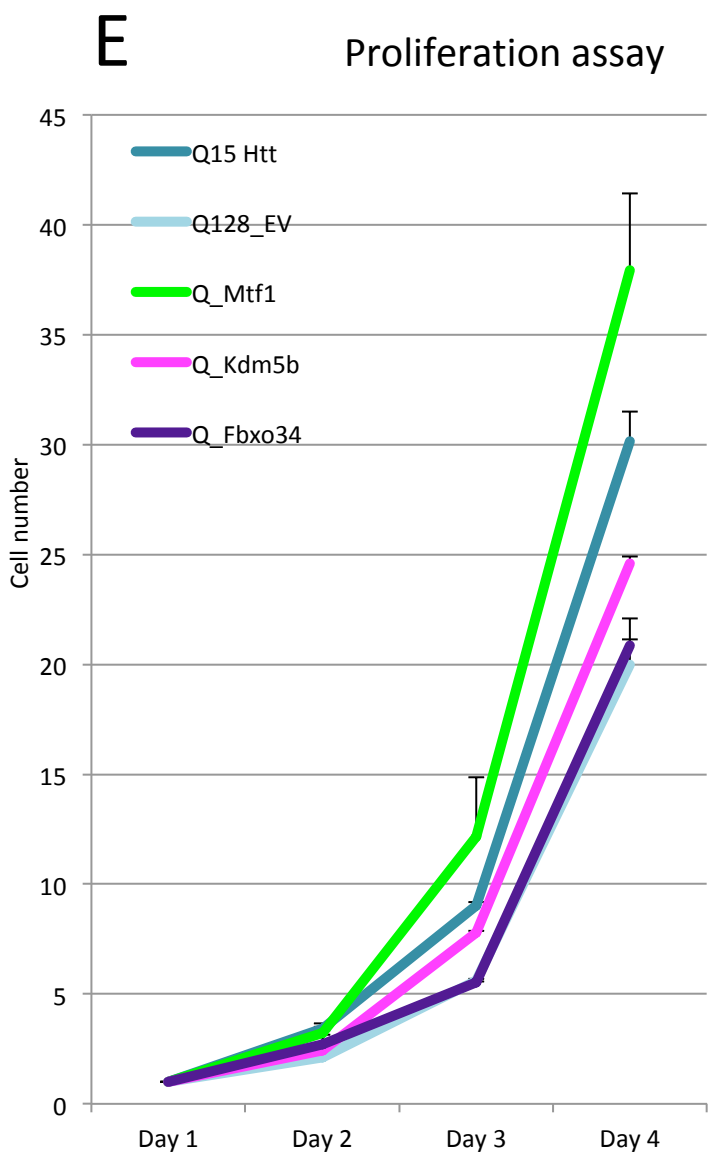
E
Proliferation assay
Cell number
45
40
35
30
25
20
15
10
5
0
Q15 Htt
Q128_EV
Q_Mtf1
Q_Kdm5b
Q_Fbxo34
Day 1
Day 2
Day 3
Day 4

Figure 17. Independent validation of candidates as genes conferring resistance to Q128 cells (2)

A and B. Crystal violet quantification showing number of surviving colonies in Q128_Mtf1, Q128_Kdm5b and Q128_Fbxo34 cells after 48hrs of treatments with MG132 (**A**) or Tamoxifen (**B**), or the vehicles DMSO and EtOH, compared to both the parental and the Q128 Htt cell lines.

Reduction in the number of cells in Q128_EV compared to Q15 cells already observed in the presence of the vehicles DMSO and EtOH, strongly exacerbate in presence of stressors.

Mtf1 and Kdm5b significantly improved cell resistance to mutant Htt, while only a modest effect was observed upon Fbxo34 overexpression.

Data are presented as mean ± standard deviation from two independent experiments, unpaired *t*-test: $*P<0.05$, $**P<0.01$, $***P<0.001$.

Figure 17

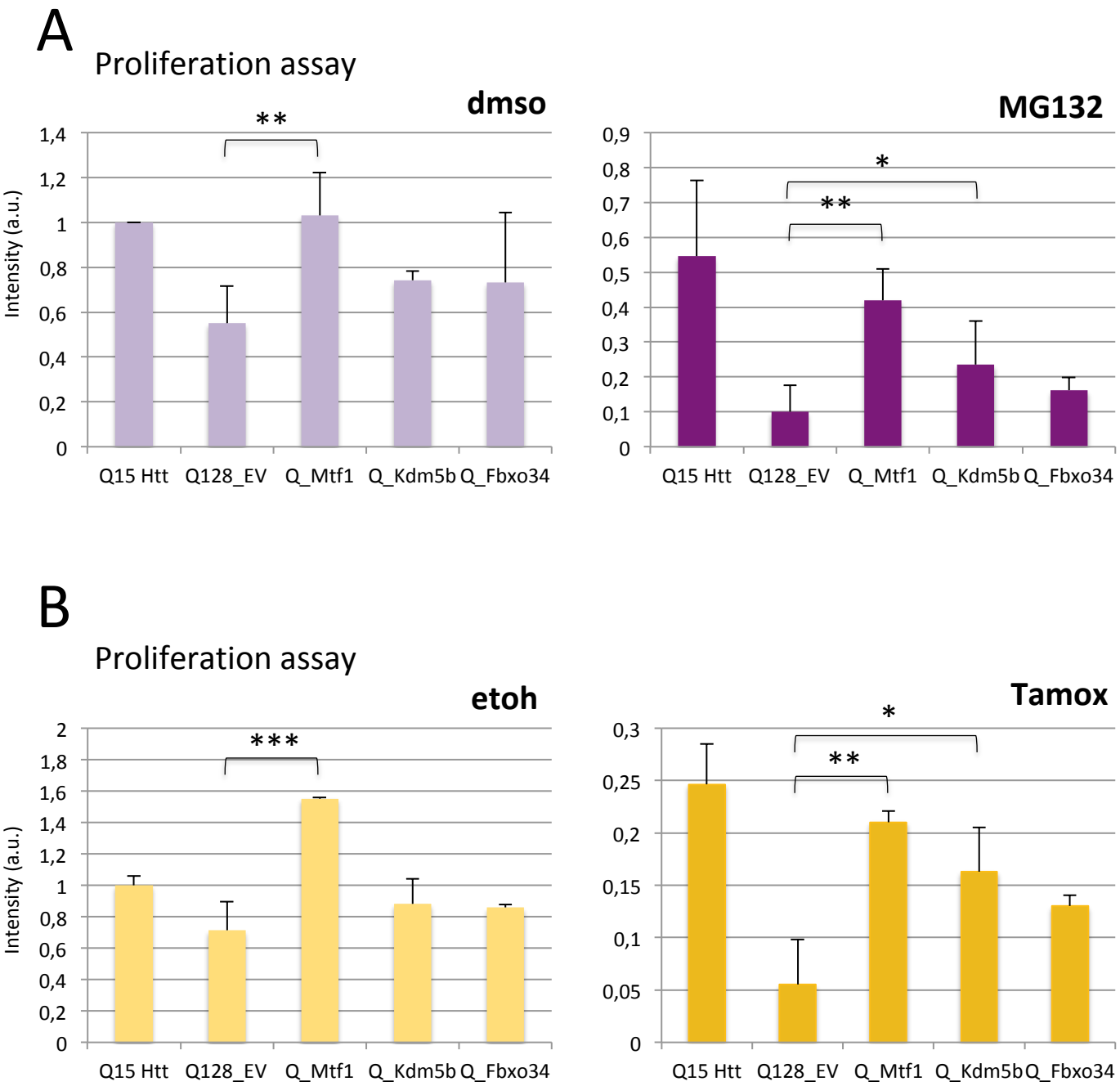
A
Proliferation assay
dmso
MG132
Intensity (a.u.)
**
*
**
1,4
1,2
1
0,8
0,6
0,4
0,2
0
0,9
0,7
0,5
0,3
0,1
Q15 Htt
Q128_EV
Q_Mtf1
Q_Kdm5b
Q_Fbxo34
B
Proliferation assay
etoh
Tamox
***
0,25
0,2
0,15
0,05

References

The Huntington's Disease Collaborative Research Group. (1993). A novel gene Benn, C. L., Sun, T., Sadri-Vakili, G., McFarland, K. N., DiRocco, D. P., Yohrling, G. J., et al. (2008). Huntingtin modulates transcription, occupies gene promoters in vivo, and binds directly to DNA in a polyglutamine-dependent manner. Journal of Neuroscience, 28(42), 10720–10733.

Bennett, E. J., Shaler, T. A., Woodman, B., Ryu, K.-Y., Zaitseva, T. S., Becker, C. H., et al. (2007). Global changes to the ubiquitin system in Huntington's disease. Nature, 448(7154), 704–708.

Biagioli, M., Ferrari, F., Mendenhall, E. M., Zhang, Y., Erdin, S., Vijayvargia, R., et al. (2015). Htt CAG repeat expansion confers pleiotropic gains of mutant huntingtin function in chromatin regulation. Human Molecular Genetics, 24(9), 2442–2457.

Carette, J.E., Raaben, M., Wong, A.C., Herbert, A.S., Obernosterer, G., Mulherkar, N., Kuehne, A.I., Kranzusch, P.J., Griffin, A.M., Ruthel, G., et al. (2011). Ebola virus entry requires the cholesterol transporter Niemann-Pick C1. Nature 477, 340-343.

Chambers I, Colby D, Robertson M, Nichols J, Lee S, et al. 2003. Functional expression cloning of Nanog, a pluripotency sustaining factor in embryonic stem cells. Cell 113(5):643–55.

Chew, S. K., Rad, R., Futreal, P. A., Bradley, A., & Liu, P. (2011). Genetic screens using the piggyBac transposon. Methods (San Diego, Calif.), 53(4), 366–371.

Conforti P, Zuccato C, Gaudenzi G, Ieraci A, Camnasio S, Buckley NJ, Mutti C, Cotelli F, Contini A, and Cattaneo E. (2013). Binding of the repressor complex REST-mSIN3b by small molecules restores neuronal gene transcription in Huntington's disease models. J. Neurochem.

Conneally PM. Huntington disease: genetics and epidemiology. (1984). Am J Hum Genet 36: 506–526.

Connelly, J.T. et al. (2010). Actin and serum response factor transduce physical cues from the microenvironment to regulate epidermal stem cell fate decisions. Nature Cell Biology Vol 12, Num 7

Davies, S. W., Turmaine, M., Cozens, B. A., DiFiglia, M., Sharp, A. H., Ross, C. A., et al. (1997). Formation of neuronal intranuclear inclusions underlies the neurological dysfunction in mice transgenic for the HD mutation. Cell, 90(3), 537–548.

DiFiglia M, Sapp E, Chase K, Schwarz C, Meloni A, Young C, Martin E, Vonsattel JP, Carraway R, Reeves SA. (1995). Huntingtin is a cytoplasmic protein associated with vesicles in human and rat brain neurons. Neuron 14: 1075–1081, 1995.

DiFiglia, M., Sapp, E., Chase, K. O., Davies, S. W., Bates, G. P., Vonsattel, J. P., & Aronin, N. (1997). Aggregation of Huntingtin in neuronal intranuclear inclusions and dystrophic neurites in brain. Science, 277(5334), 1990–1993.

Dunah, A. W., Jeong, H., Griffin, A., Kim, Y.-M., Standaert, D. G., Hersch, S. M., et al. (2002). Sp1 and TAFII130 transcriptional activity disrupted in early Huntington's disease. Science, 296(5576), 2238–2243.

Duyao MP, Auerbach AB, Ryan A, Persichetti F, Barnes GT, McNeil SM, Ge P, Vonsattel JP, Gusella JF, Joyner AL. (1995). Inactivation of the mouse Huntington's disease gene homolog Hdh. Science 269: 407– 410.

Ellerby, L. M., Andrusiak, R. L., Wellington, C. L., Hackam, A. S., Propp, S. S., Wood, J. D., et al. (1999). Cleavage of atrophin-1 at caspase site aspartic acid 109 modulates cytotoxicity. The Journal of Biological Chemistry, 274(13), 8730–8736.

Evans MJ, Kaufman MH. (1981). Establishment in culture of pluripotential cells from mouse embryos. Nature 292(5819):154–56

Giorgini, F., Guidetti, P., Nguyen, Q., Bennett, S.C., and Muchowski, P.J. (2005). A genomic screen in yeast implicates kynurenine 3-monooxygenase as a therapeutic target for Huntington disease. Nat Genet *37*, 526-531.

Goldberg, Y. P., Nicholson, D. W., Rasper, D. M., Kalchman, M. A., Koide, H. B., Graham, R. K., et al. (1996). Cleavage of huntingtin by apopain, a proapoptotic cysteine protease, is modulated by the polyglutamine tract. Nature Genetics, 13(4), 442–449.

Guo, G., Wang, W., and Bradley, A. (2004). Mismatch repair genes identified using genetic screens in Blm-deficient embryonic stem cells. Nature 429, 891–895.

Guo G, Yang J, Nichols J, Hall JS, Eyres I, et al. 2009. Klf4 reverts developmentally programmed restrictionof ground state pluripotency. Development 136(7):1063–69.

Guo, G., and Smith, A. (2010). A genome-wide screen in EpiSCs identifies Nr5a nuclear receptors as potent inducers of ground state pluripotency. Development 137, 3185-3192.

Hansen, G. M., Markesich, D. C., Burnett, M. B., Zhu, Q., Dionne, K. M., Richter, L. J., Finnell, R. H., Sands, A. T., Zambrowicz, B. P., and Abuin, A. (2008). Large-scale gene trapping in C57BL/6N mouse embryonic stem cells. Genome Res. 18, 1670–1679.

HD iPSC Consortium (2012). Induced pluripotent stem cells from patients with Huntington's disease show CAG-repeat- expansion-associated phenotypes. Cell Stem Cell 11, 264-278.

Hilditch-Maguire, P., Trettel, F., Passani, L. A., Auerbach, A., Persichetti, F., & MacDonald, M. E. (2000). Huntingtin: an iron-regulated protein essential for normal nuclear and perinuclear organelles. Human Molecular Genetics, 9(19), 2789–2797.

Hoffner, G., Island, M. L., & Djian, P. (2005). Purification of neuronal inclusions of patients with Huntington's disease reveals a broad range of N-terminal fragments of expanded huntingtin and insoluble polymers. Journal of Neurochemistry, 95(1), 125–136.

Ismailoglu, I., Chen, Q., Popowski, M., Yang, L., Gross, S. S., & Brivanlou, A. H. (2014). Huntingtin protein is essential for mitochondrial metabolism, bioenergetics and structure in murine embryonic stem cells. Developmental Biology, 391(2), 230–240.
Jonson, I., Ougland, R., Klungland, A., & Larsen, E. (2013). Oxidative stress causes DNA triplet expansion in Huntington's disease mouse embryonic stem cells. Stem Cell Research, 11(3), 1264–1271.

Ju, J.-S., Miller, S. E., Jackson, E., Cadwell, K., Piwnica-Worms, D., & Weihl, C. C. (2014). Quantitation of selective autophagic protein aggregate degradation in vitro and in vivo using luciferase reporters. Autophagy, 5(4), 511–519. http://doi.org/10.4161/auto.5.4.7761

Kim, Y. J., Yi, Y., Sapp, E., Wang, Y., Cuiffo, B., Kegel, K. B., et al. (2001). Caspase 3-cleaved N-terminal fragments of wild-type and mutant huntingtin are present in normal and Huntington's disease brains, associate with membranes, and undergo calpain-dependent proteolysis.

Leeb, M., Dietmann, S., Paramor, M., Niwa, H., & Smith, A. (2014). Genetic Exploration of the Exit from Self-Renewal Using Haploid Embryonic Stem Cells. Cell Stem Cell, 14(3), 385–393.

Li, M.A., Pettitt, S.J., Yusa, K., and Bradley, A. (2010). Genome-wide forward genetic screens in mouse ES cells. Methods Enzymol. 477, 217–242.

Liang, Q., Kong, J., Stalker, J., and Bradley, A. (2009). Chromosomal mobilization and reintegration of Sleeping Beauty and piggyBac transposons. Genesis 47, 404–408.

Lo Sardo, V., Zuccato, C., Gaudenzi, G., Vitali, B., Ramos, C., Tartari, M., Myre, M.A., Walker, J.A., Pistocchi, A., Conti, L., et al. (2012). An evolutionary recent neuroepithelial cell adhesion function of huntingtin implicates ADAM10-Ncadherin. Nat Neurosci 15, 713-721.

Martello G and Smith. (2014). The Nature of Embryonic Stem Cells. Annu. Rev. Cell Dev. Biol. 2014. 30:647–75.

Martin GR. (1981). Isolation of a pluripotent cell line from early mouse embryos cultured in medium conditioned by teratocarcinoma stem cells. Proc. Natl. Acad. Sci. USA 78(12):7634–38.

Mihiro S., et al. (2017). Arid1b Haploinsufficiency Causes Abnormal Brain Gene Expression and Autism-Related Behaviors in Mice, 18(9), 1872.

Mikkers, H., Allen, J., Knipscheer, P., Romeijn, L., Hart, A., Vink, E., Berns. A. (2002). Nat. Genet. 32153–159.

Miralles, F., Posern, G., Zaromytidou,1 A., Treisman R. (2003). Actin Dynamics Control SRF Activity by Regulation of Its Coactivator MAL.. Cell, Vol. 113, 329–342.

Nagl, N. G., Wang, X., Patsialou, A., Van Scoy, M., & Moran, E. (2007). Distinct mammalian SWI/SNF chromatin remodeling complexes with opposing roles in cell-cycle control. The EMBO Journal, 26(3), 752–763.

Nasir, J. (1995). Targeted disruption of the Huntington's disease gene results in embryonic lethality and behavioral and morphological changes in heterozygotes. Cell, 81(5), 811–823.

Niclis, J. C. (2009). Human embryonic stem cell models of Huntington disease. Reproductive BioMedicine Online, 19(1), 106–113.

Nollen, E.A.A., Garcia, S.M., van Haaften, G., Kim, S., Chavez, A., Morimoto, R.I., and Plasterk, R.H.A. (2004). Genome- wide RNA interference screen identifies previously undescribed regulators of polyglutamine aggregation. Proc Natl Acad Sci USA 101, 6403-6408.

Nucifora, F.C., Sasaki, M., Peters, M.F., Huang, H., Cooper, J.K., Yamada, M., Takahashi, H., Tsuji, S., Troncoso, J., Dawson, V.L., et al. (2001). Interference by huntingtin and atrophin-1 with cbp-mediated transcription leading to cellular toxicity. Science 291, 2423-2428.

Panov, A. V., Gutekunst, C.-A., Leavitt, B. R., Hayden, M. R., Burke, J. R., Strittmatter, W. J., & Greenamyre, J. T. (2002). Early mitochondrial calcium defects in Huntington's disease are a direct effect of polyglutamines. Nature Neuroscience, 5(8), 731–736.

Potter, C.J., Luo L. (2010). Splinkerette PCR for mapping transposable elements in Drosophila. PLoS One. 4, e10168.

Reiner, A., Albin, R. L., Anderson, K. D., D'Amato, C. J., Penney, J. B., & Young, A. B. (1988). Differential loss of striatal projection neurons in Huntington disease. Proceedings of the National Academy of Sciences, 85(15), 5733–5737.

Rigamonti, D., Bauer, J.H., De-Fraja, C., Conti, L., Sipione, S., Sciorati, C., Clementi, E., Hackam, A., Hayden, M.R., Li, Y., et al. (2000). Wild-type huntingtin protects from apoptosis upstream of caspase-3. J Neurosci 20, 3705-3713.

Rigamonti D, Bolognini D, Mutti C, Zuccato C, Tartari M, Sola F, Valenza M, Kazantsev AG, Cattaneo E. (2007). Loss of huntingtin function complemented by small molecules acting as repressor element 1/neuron restrictive silencer element silencer modulators. J Biol Chem 282: 24554 –24562.

Ross, C.A., and Tabrizi, S.J. (2011). Huntington's disease: from molecular pathogenesis to clinical treatment. Lancet Neurol 10, 83-98.

Saini, N., Georgiev, O., & Schaffner, W. (2011). The parkin Mutant Phenotype in the Fly Is Largely Rescued by Metal-Responsive Transcription Factor (MTF-1). Molecular and Cellular Biology, 31(10), 2151–2161.

Scaramuzzino C. et al. (2015). Protein arginine methyltransferase 6 enhances polyglutamine-expanded androgen receptor function and toxicity in spinal and bulbar muscular atrophy. 85(1), 88–100.

Sepers, M. D., & Raymond, L. A. (2014). Mechanisms of synaptic dysfunction and excitotoxicity in Huntington's disease. Drug Discovery Today, 19(7), 990–996.

Sipione S, Cattaneo E. Modeling Huntington's disease in cells, flies, and mice. (2001). Mol Neurobiol 23: 21–51.

Sugars, K. L., & Rubinsztein, D. C. (2003). Transcriptional abnormalities in Huntington disease. Trends in Genetics, 19(5), 233–238.

The Huntington's Disease Collaborative Research Group. (1993). A novel gene containing a trinucleotide repeat that is expanded and unstable on Huntington"s disease chromosomes. Cell *72*, 971-983.

Trombly, M. I., Su, H., and Wang, X. (2009). A genetic screen for components of the mammalian RNA interference pathway in Bloom-deficient mouse embryonic stem cells. Nucleic Acids Res. 37, e34.

Varma H, Voisine C, DeMarco CT, Cattaneo E, Lo DC, Hart AC, Stockwell BR. (2007). Selective inhibitors of death in mutant huntingtin cells. Nat Chem Biol 3: 99–100.

Vartiainen, M.K. et al. (2007). Nuclear Actin Regulates Dynamic Subcellular Localization and Activity of the SRF Cofactor MAL. Science 316, 1749.

Verllinsky Y (2005). Human embryonic stem cell lines with genetic disorders. Reproductive BioMedicine Online, 10(1), 105–110.

Vierbuchen, T., Ostermeier, A., Pang, Z. P., Kokubu, Y., Südhof, T. C., & Wernig, M. (2010). Direct conversion of fibroblasts to functional neurons by defined factors. Nature, 463(7284), 1035–1041.

Wang, W., and Bradley, A. (2007). A recessive genetic screen for host factors required for retroviral infection in a library of insertionally mutated Blm-deficient embryonic stem cells. Genome Biol. 8, R48.

Wang, W., Lin, C., Lu, D., Ning, Z., Cox, T., Melvin, D., Wang, X., Bradley, A., and Liu, P. (2008). Chromosomal transposition of PiggyBac in mouse embryonic stem cells. Proc. Natl. Acad. Sci. USA 105, 9290–9295.

Wellington, C. L., Singaraja, R., Ellerby, L., Savill, J., Roy, S., Leavitt, B., et al. (2000). Inhibiting caspase cleavage of huntingtin reduces toxicity and aggregate formation in neuronal and nonneuronal cells. The Journal of Biological Chemistry, 275(26), 19831–19838.

Wellington CL, Ellerby LM, Gutekunst CA, Rogers D, Warby S, Graham RK, Loubser O, van Raamsdonk J, Singaraja R, Yang YZ, Gafni J, Bredesen D, Hersch SM, Leavitt BR, Roy S, Nicholson DW, Hayden MR. (2002). Caspase cleavage of mutant huntingtin precedes neurodegeneration in Huntington's disease. J Neuro- sci 22: 7862–7872.

Wu, S. C., Meir, Y. J., Coates, C. J., Handler, A. M., Pelczar, P., Moisyadi, S., and Kaminski, J. M. (2006). piggyBac is a flexible and highly active transposon as compared to sleeping beauty, Tol2, and Mos1 in mammalian cells. Proc. Natl. Acad. Sci. USA 103, 15008–15013.

Ying QL, Wray J, Nichols J, Batlle-Morera L, Doble B, et al. (2008). The ground state of embryonic stem cell self-renewal. Nature 453(7194):519–23

Yusa, K., Rad, R., Takeda, J., and Bradley, A. (2009). Generation of transgene-free induced pluripotent mouse stem cells by the piggyBac transposon. Nat. Methods 6, 363–369.

Zeitlin, S., Liu, J.-P., Chapman, D. L., Papaioannou, V. E., & Efstratiadis, A. (1995). Increased apoptosis and early embryonic lethality in mice nullizygous for the Huntington's disease gene homologue. Nature Genetics, 11(2), 155–163.

Zuccato, C., Ciammola, A., Rigamonti, D., Leavitt, B. R., Goffredo, D., Conti, L., et al. (2001). Loss of Huntingtin-Mediated BDNF Gene Transcription in Huntington's Disease. Science, 293(5529), 493–498.

Zuccato, C., Valenza, M., and Cattaneo, E. (2010). Molecular mechanisms and potential therapeutical targets in Huntington's disease. Physiol. Rev. 90, 905-981.

Zwilling, D., Huang, S.-Y., Sathyasaikumar, K.V., Notarangelo, F.M., Guidetti, P., Wu, H.-Q., Lee, J., Truong, J., Andrews- Zwilling, Y., Hsieh, E.W., et al. (2011). Kynurenine 3-monooxygenase inhibition in blood ameliorates neurodegeneration. Cell *145*, 863-874.